



The Aura Mission

Project Science Team

M. Schoeberl, A. Douglass, J. Joiner
NASA/GSFC

Ozone Monitoring Instrument

P. Levelt, KNMI, NL
J. Tamminen, FMI, FI
P.K. Bhartia, NASA/GSFC

High Resolution Dynamics Limb Sounder

J. Gille
NCAR & U. of Colorado
J. Barnett
Oxford Univ., UK

Tropospheric Emission Spectrometer

R. Beer, A. Eldering
NASA/JPL

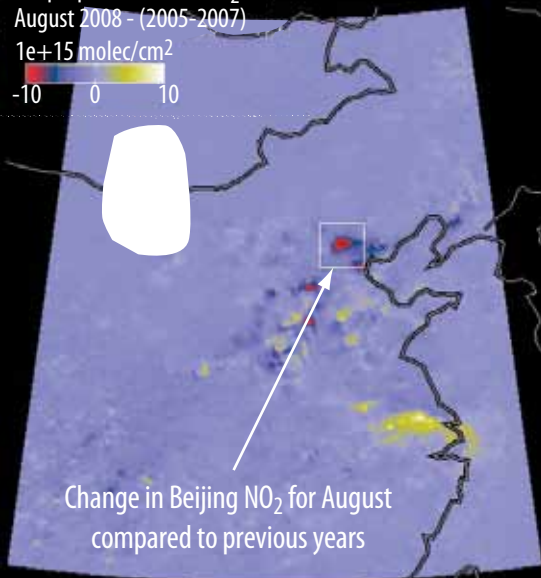
Microwave Limb Sounder

N. Livesey
NASA/JPL



The September 1, 2005 ozone hole (top) as measured by the OMI instrument on Aura. Below, ClO (left) and HCl (right) maps from MLS for the same day showing chlorine activation and reservoir depletion.

Tropospheric Column NO₂
August 2008 - (2005-2007)
1e+15 molec/cm²
-10 0 10



Changes in NO₂ over Beijing during the 2008 Olympics show the impact of pollution reduction compared to previous years.

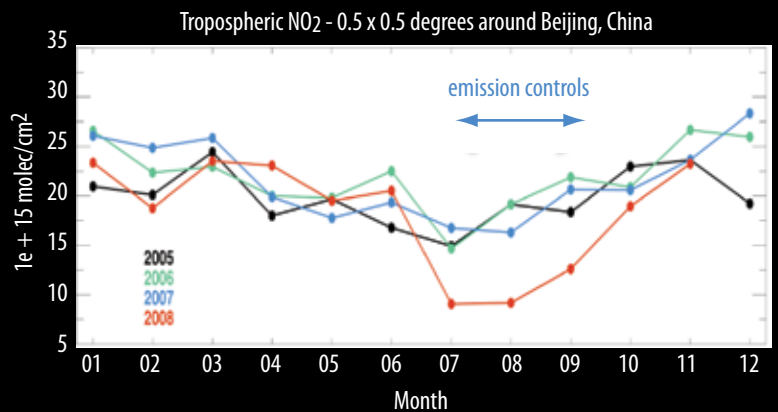


TABLE OF CONTENTS

Executive Summary 1

1.0 Introduction 1

2.0 Status of Aura Instruments & Core Products 3

 2.1 Microwave Limb Sounder (MLS) 3

 2.2 Ozone Monitoring Instrument (OMI) 3

 2.3 Tropospheric Emission Spectrometer (TES) 4

 2.4 High Resolution Dynamics Limb Sounder (HIRDLS) 4

3.0 Aura Prime Mission Accomplishments 5

 3.1 Is the Ozone Layer Changing as Expected? 5

 3.1.1 Trends in Stratospheric Trace Gases 5

 3.1.2 Ozone Hole Photochemistry 6

 3.1.3 Ozone photochemistry and middle and low latitude ozone depletion 7

 3.1.4 Summary 8

 3.2 What are the Processes that Control Tropospheric Pollutants? 8

 3.2.1 Sulfur Dioxide (SO₂) from OMI and TES 9

 3.2.2 Nitrogen Dioxide (NO₂) from OMI 9

 3.2.3 Carbon Monoxide (CO) from MLS and TES 9

 3.2.4 Tropospheric O₃ and VOCs from TES, OMI, and MLS 10

 3.2.5 Summary of Processes that Control Tropospheric Pollutants 11

 3.3 What are the Roles of Upper Tropospheric Aerosols, Cirrus Clouds, Water Vapor, and Ozone in Climate Change? . 11

 3.3.1 Clouds, H₂O, HDO and aerosols 11

 3.3.2 Chemistry and Climate 12

 3.3.3 Summary 13

 3.4 A-Train Science 14

 3.5 Relevance to Modeling and Prediction 14

4.0 The Aura Extended Mission Proposal 15

 4.1 Is the O₃ layer changing as expected? 15

 4.2 What are the Processes that Control Tropospheric Pollutants? 16

 4.3 What are the Roles of UT Aerosols, Water Vapor and Ozone in Climate Change? 17

 4.3.1 Water vapor, clouds and aerosols issues 17

 4.3.2 Changes in Stratospheric Dynamics 17

 4.3.3 Upper Tropospheric Radiative Forcing 18

 4.3.4 Climate impact of volcanoes 18

5.0 Proposed Aura Extended Mission Implementation Plan 18

 5.1 Microwave Limb Sounder (MLS) 19

 5.1.1 Data Products 19

 5.1.2 Methyl chloride 19

 5.1.3 Products supporting MLS data 19

 5.1.4 Improved Cloud and Cloudy-sky Products 19

 5.1.5 Proposed V5 Algorithm 20

 5.1.6 New Approach for ‘Noisy Products’ (Optimal Budget) 20

 5.2 Ozone Monitoring Instrument (OMI) 20

 5.2.1 Instrument Characterization 20

 5.2.2 Maintenance and Improvement of TOMS Heritage Products 20

 5.2.3 UV Radiative Transfer Development 21

 5.2.4 Specialized Ancillary Datasets 21

 5.3 Tropospheric Emission Spectrometer (TES) 21

 5.3.1 Data Products 21

 5.3.2 Proposed Algorithm Improvements 21

 5.3.3 Transitioning TES L2 Products 21

 5.4 High Resolution Dynamics Limb Sounder (HIRDLS) 22

5.4.1 Data Products 22

5.4.2 Specific Proposed Algorithm Improvements. 22

5.4.3 Case of Chopper Restarting 23

5.5 Proposed Instrument Combined Products 23

5.5.1 Ozone Profiles with Boundary Layer Sensitivity from TES + OMI (Optimal Budget). 24

5.5.2 Integrated CO Profiles from Lower Troposphere to Mesosphere from TES + MLS (Optimal Budget). 24

5.5.3 Ice Water Content of Cirrus Particles (HIRDLS + MLS) 24

5.6 Validation Needs 24

6.0 Applications 25

6.1 OMI NRT Products for Operational Applications 25

6.2 MLS NRT Products for Operational Applications 26

7.0 Aura Technical Status of Mission Components 26

7.1 Mission Operations Overview and Status 26

7.1.1 Flight Operations 26

7.1.2 Data Capture and Level 0 Processing 26

7.1.3 Afternoon Constellation Coordination 27

7.1.4 EOS Mission Operations Ground System. 27

7.1.5 Management of Flight Operations and Ground System 28

7.2 Spacecraft Status and Health. 29

7.2.1 Propulsion Subsystem 29

7.2.2 Electrical Power Subsystem (EPS). 29

7.2.3 Guidance, Navigation, & Control (GN&C) Subsystem. 29

7.2.4 Communications Subsystem 29

7.2.5 Command & Data Handling (C&DH) Subsystem 29

7.2.6 Thermal Control Subsystem. 29

7.2.7 Summary 29

7.2.8 End of Life Approach 30

7.3 Instruments 30

7.3.1 HIRDLS Status and Health. 30

7.3.2 MLS Status and Health 30

7.3.3 OMI Status and Health. 31

7.3.4 TES Status and Health 31

8.0 Aura Budget Narratives 32

8.1 MLS Budget Narrative. 32

8.1.1 In Guide Budget 32

8.1.2 In-kind and Other Funding. 32

8.1.3 Optimal Budget. 32

8.2 HIRDLS Budget Narrative 33

8.2.1 In Guide Budget 33

8.2.2 Optimal Budget. 33

8.3 OMI Budget Narrative. 33

8.3.1 In Guide Budget 33

8.3.2 Optimal budget. 34

8.4 TES Budget Narrative 34

8.4.1 In Guide Budget 34

8.4.2 In-kind Funding 34

8.4.3 Optimal budget. 34

8.5 ESMO Budget Narrative 35

9.0 OMB Efficiency Metric. 35

10.0 Summary 36

Appendix A Mission Data Product Inventory. 37

Appendix A1 45

Appendix B Mission Budget 46

Appendix C - Acronym List 56

Appendix D - Cited References 60

Appendix E 72

E.0 Spacecraft and Instrument Engineering Trend Plots 72

 E.1 Spacecraft Subsystem Performance Engineering Plots 72

 E.1.1 Propulsion Subsystem 72

 E.1.2 Electrical Power Subsystem (EPS). 72

 E.1.3 Guidance, Navigation, & Control (GN&C) Subsystem 76

 E.1.4 Command & Data Handling (C&DH) Subsystem 76

 E.1.5 Communications Subsystem 77

 E.1.6 Thermal Control Subsystem 78

 E.1.7 Aura Reliability and Lifetime Estimates: 78

 E.2 Results of Aura Review to Ensure Compliance with Recommendations from the Mars Global Surveyor Operatio
Review Board 79

 E.3 Process Improvement Initiatives 80

 E.4 Instrument Science and Operations Engineering Trend Plots 81

 E.4.1 Microwave Limb Sounder (MLS) Engineering Trend Plots 81

 E.4.2 Tropospheric Emission Spectrometer (TES):Engineering Trend Plots 81

 E.4.3 Ozone Monitoring Instrument (OMI) Engineering Trend Plots 83

EXECUTIVE SUMMARY

The Aura satellite, launched July 15, 2004, carries four instruments (the Ozone Monitoring Instrument (OMI), the High Resolution Dynamics Limb Sounder (HIRDLS), the Microwave Limb Sounder (MLS), and the Tropospheric Emission Spectrometer (TES)) built through international collaborations of NASA (USA), NIVR (The Netherlands), FMI (Finland), and NERC (UK). Aura's unique measurements of a large number of trace gases in the stratosphere and troposphere have led to many important scientific discoveries and published studies. There are currently no plans to duplicate or replace Aura's capabilities with successor NASA missions, and only a very limited number of Aura measurements will be picked up by NPP/NPOESS and the ESA EarthWatch program.

Starting a few weeks after launch, Aura instruments began measuring a suite of chemical constituents at high vertical and horizontal resolution throughout the atmosphere to address three principal science questions.

- *Is the ozone layer changing as expected?*
- *What are the processes that control tropospheric pollutants?*
- *What are the roles of upper tropospheric aerosols, water vapor, and ozone in climate change?*

The four Aura instruments have made nearly continuous measurements during the nearly five-year period since launch. All instruments with the exception of HIRDLS are operating normally. The HIRDLS chopper motor stalled in March 2008. Efforts to restart the chopper are ongoing, and the motor may yet restart. The Aura spacecraft has not experienced a safe mode, continues to perform extremely well, and has sufficient propellant for at least 8 more years of orbital maneuvers. Power resources are robust and all spacecraft subsystems are expected to function nominally during FY10-FY13. OMI and MLS are expected to operate through FY13 and TES is expected to operate until at least 2011.

Aura has met its mission success criteria. All the instruments have submitted the data to the NASA DISC and nearly all the data have been validated. All the instrument teams have released reprocessed data using updated algorithms. The scientific output from the Aura mission is significant. The total number of publications using Aura data grew from 10 in 2005 to about 90 in 2008, with 353 papers published in total between launch and the start of 2009. These papers describe in exquisite new detail chemical and physical processes in the stratosphere and troposphere. Discoveries from Aura include the first global inventory of SO₂ emissions, observations of the trapping and long-range transport of air pollution, insights into the water cycle through new measurements of isotopic water, the first daily global estimates of tropospheric ozone and its role as a greenhouse gas, first measurements of the hydroxyl radical throughout the stratosphere, identification of new 'tape recorder' signatures in the tropical lower stratosphere, identification of filamentary trace gas structures in the lower stratosphere, and more, as described in this document.

The Near-Real-Time (NRT) products of Aura OMI and MLS are increasingly valued by the operational community.

The OMI ozone NRT product is delivered to ECMWF and NOAA for incorporation into weather forecast models, and the USGS uses OMI SO₂ and aerosol index for tracking volcanic plumes for aircraft hazard warnings. MLS stratospheric ozone profiles have been shown to lead to assimilation model improvements (including NASA's GEOS-5, the Navy's NOGAPS-Alpha, ECMWF, NOAA NCEP). An NRT MLS ozone and temperature product has recently been developed and is being used with OMI data to produce NRT tropospheric ozone residual.

The Aura observations are a unique resource for the atmospheric science community and have led to important advances in our understanding of climate, air quality and ozone layer chemistry and dynamics. However, as detailed in this proposal, a longer record of observations, incorporating a greater range of variability (both natural and anthropogenic) is needed to improve and validate our understanding of the Earth system. Specifically, observations are required to understand the global impact of changing pollution emissions, with emissions from Asia and Siberian forest fires set to increase, concurrent with decreasing European emissions and increased biomass burning due to changes in land use in the tropics. A long record of observations of the impact of climate-related phenomena such as El Niño Southern Oscillation (ENSO) and the Madden-Julian Oscillation (MJO) on atmospheric composition is critical to our understanding of climate feedbacks, and how future climate variations will affect air quality, hydrology, and the ozone layer. Extended mission Aura observations are also essential to the continuation of established and valuable long term records of atmospheric composition. Additional activities proposed here beyond continued observations include improvements to current Aura products, and the transitioning of research products to operational processing. Also proposed are augmented cloud products that complement other A-train cloud observations, and multi-instrument versions of established Aura products, offering improved vertical resolution and coverage.

1.0 INTRODUCTION

Aura, the third of the large Earth Observing System (EOS) observatories, was launched July 15, 2004 into a 705-km sun-synchronous polar orbit with a 98° inclination and an ascending-node equator-crossing time of 13:45±15 min. The design life is five years with an operational goal of six years.

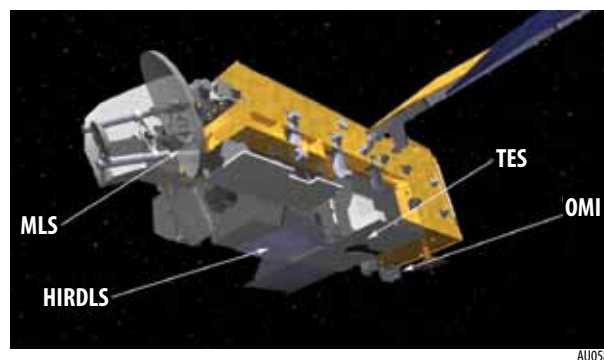


Figure 1: The Aura spacecraft showing positions of instruments.

Aura has four instruments: the High Resolution Dynamics Limb Sounder (HIRDLS), the Microwave Limb Sounder (MLS), the Ozone Monitoring Instrument (OMI) and the Tropospheric Emission Spectrometer (TES). **Figure 1** shows the instrument positions. The measurements made by the Aura instruments are highly complementary, and the positioning of these instruments on the spacecraft was intentionally designed to maximize their cross-observational capability. Looking forward, MLS makes limb measurements in the direction of flight, OMI and TES make nadir soundings of the same air mass as the spacecraft flies over. In Limb mode TES makes measurements looking backward, and HIRDLS measures profiles with high vertical resolution at 47° from the satellite track. **Figure 2** shows the measurement strategy.

Starting a few weeks after launch, Aura instruments have measured a suite of chemical constituents at high vertical

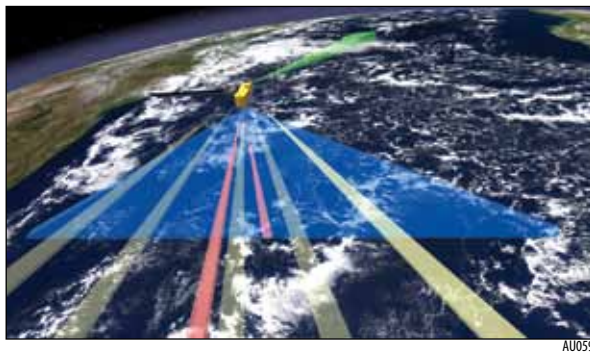


Figure 2: The look positions of the various Aura instruments, green, MLS; red TES (limb and nadir); blue (OMI), yellow HIRDLS. Due to a launch accident, HIRDLS can only sample along the bright yellow direction shown above. The limitation on the HIRDLS measurements is discussed in Section 2.4.

and horizontal resolution throughout the atmosphere to address three principal science questions:

- *Is the ozone layer changing as expected?*
- *What are the processes that control tropospheric pollutants?*
- *What are the roles of upper tropospheric aerosols, water vapor, and ozone in climate change?*

These questions are directly related to the first research objective in the NASA strategic plan: Understand and improve predictive capability for changes in the stratospheric ozone layer, climate forcing and air quality associated with changes in atmospheric composition. Aura also fulfills Congressional Mandate and Clean Air Act requirements (1975, 1990) for NASA to monitor the state of the stratospheric ozone layer. Aura measurements provide unprecedented insights into the chemical and dynamical processes associated with our atmosphere. Besides this introduction, the science section is divided into the following subsections: (2) Status of Aura Instruments and Core Products; (3) Aura Prime Mission Accomplishments; (4) The Aura extended Mission Proposal; (5) Proposed Aura Extended Mission Implementation Plan; (6) Applications; (7) Aura Technical Status of Mission Components; (8) Aura Budget Narratives; (9) OMB Efficiency Metric; (10) Summary. The proposal includes four required appendices: (A) Mission Data Product Inventory; (B) Mission budget; (C) Acronym list; (D) Cited references. We include two additional appendices: (E) engineering data and (A1) a list of ROSES proposals that produce core products for the Ozone Monitoring Instrument.

The Aura Project and Mission Operations are managed by Goddard Space Flight Center. Data archiving for three of the four instruments (MLS, TES, OMI) also takes place at the Goddard Earth Sciences Data and Information Services Center (GES DISC). TES data is archived at the NASA

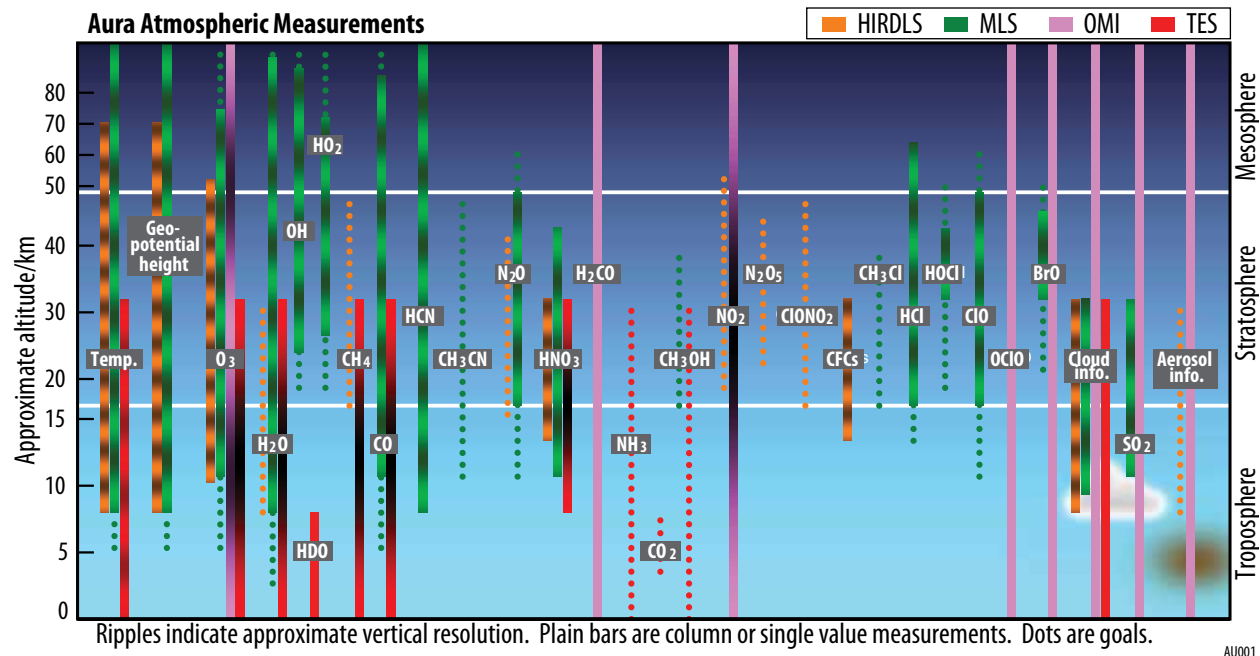


Figure 3: Schematic of measurements from the Aura instruments.

Table 1: MLS Core Product Information (for version 2 data)

Product	Useful Range	Estimated Accuracy	Vert. Res. (km)	Validation papers
Temperature	0.001-315 hPa	± 2 K for 316-3 hPa ± 5 K for 2-0.001 hPa	3-6 7-15	<i>Schwartz et al.</i> [2008]
Geopot. Hght	0.001-315 hPa	< 150 m for p > 0.01 hPa		<i>Schwartz et al.</i> [2008]
O ₃	Strat & above 0.02-100 hPa UT: 100-215 hPa	20-35 % for p < 0.2 hPa 3-10 % for 0.2-100 hPa ~ 20 ppbv + 5-20 %	4-6 3 3	<i>Froidevaux et al.</i> [2008a] <i>Jiang et al.</i> [2007] <i>Livesey et al.</i> [2008]
CO	0.002-100 hPa UT: 150-215 hPa	10-50% 150 hPa: 30 ppbv + 30% 215 hPa: 40 ppbv +100% (high)	4-5 3-9	<i>Pumphrey et al.</i> [2007] <i>Livesey et al.</i> [2008]
H ₂ O	0.002-0.1 hPa 0.2-70 hPa UT/LS: 80-315 hPa	8-35 % 4-9 % 7-25 %	12-16 3-7 1.5-3.5	<i>Lambert et al.</i> [2007] <i>Read et al.</i> [2007]
Rel. Humid.	UT/LS: 80-315 hPa	20-35 %	4-6	<i>Read et al.</i> [2007]
N ₂ O	1-100 hPa	9-25 %	4-6	<i>Lambert et al.</i> [2007]
HNO ₃	3-215 hPa	~10-30 %	3.5-5	<i>Santee et al.</i> [2007]
HCl	0.15-20 hPa 30-100 hPa	5-10 % 10->100 % a (0.2-0.4 ppbv)	3-6	<i>Froidevaux et al.</i> [2008b]
ClO	1-100 hPa	10-20%; negative bias of 0.1-0.4 ppbv for p > 40 hPa	3-4.5	<i>Santee et al.</i> [2008b]
HOCl	2-10 hPa	30-100 % for zonal mean	6	<i>Livesey et al.</i> [2007]
BrO	3-10 hPa	20 % (for zonal mean)	5-6	<i>Kovalenko et al.</i> [2007]
OH	0.003-30 hPa	15%	2.5-5	<i>Pickett et al.</i> [2008]
HO ₂	0.03-20 hPa	20% (for zonal mean)	5-16	<i>Pickett et al.</i> [2008]
HCN	0.1-10 hPa	50% (for zonal mean)	10-12	<i>Pumphrey et al.</i> [2006]
cloud ice water content	80-215 hPa	100% for (IWC < 50 mg/m ³)	4	<i>Wu et al.</i> [2008b]

Langley Atmospheric Science Data Center. JPL operates the TES and MLS instruments while the University of Colorado and Oxford University operate HIRDLS. The OMI instrument, a contribution from the Netherlands and Finland, is operated by KNMI in the Netherlands. After acquiring the raw data from the spacecraft, the individual instrument teams process the data at their local institutions except for OMI where processing also takes place at Goddard Space Flight Center as part of the US OMI contribution. The annual Aura Science Team is hosted in rotation by the instrument institutions.

2.0 STATUS OF AURA INSTRUMENTS & CORE PRODUCTS

The Aura instruments make complementary measurements of a comprehensive suite of molecules, which in combination give complete vertical coverage of key species from the lower troposphere to the mesosphere. An overview of each instrument and its status follows. Details are found in the technical section (Section 7). **Figure 3** shows the coverage of Aura measurements with the ripples indicating the vertical resolution. This figure also shows the complementary nature of the Aura instrument measurements and the selective redundancy.

2.1 Microwave Limb Sounder (MLS)

MLS a limb scanning emission microwave radiometer that can measure stratospheric and upper tropospheric temperature and constituents. MLS operates in the GHz and THz frequency ranges. MLS also measures cloud ice content along with upper tropospheric water vapor and

other species in the presence of tropical clouds. MLS products, their useful range, accuracy and vertical resolution are shown in **Table 1** along with their validation papers. The MLS data quality document can be found at <http://mls.jpl.nasa.gov/data/datadocs.php>. MLS has performed well since launch. However one of the measurement bands (13- the primary HCl band) is currently turned on only sparingly due to degradation of the electronics and a desire to conserve lifetime. Further information concerning the health of MLS is given in Section 7.3.2.

2.2 Ozone Monitoring Instrument (OMI)

The Netherlands' Agency for Aerospace Programs (NIVR), in collaboration with the Finnish Meteorological Institute (FMI), contributed OMI to the Aura mission. KNMI, the Dutch meteorological agency is the PI institute for OMI. OMI continues the total O₃ record begun by the Total Ozone Mapping Spectrometer (TOMS) in 1979. OMI measures other atmospheric parameters related to composition and climate listed in **Table 2** [Levell et al., 2006]. The OMI data guide and validation information can be found at <http://disc.sci.gsfc.nasa.gov/Aura/documentation/index.shtml> and <http://www.knmi.nl/omi/research/calibration/index.html>

OMI employs hyperspectral imaging to observe solar backscatter radiation in the visible and ultraviolet. The Earth is viewed in 740 wavelength bands from 270-500 nm with a spectral resolution of ~0.5 nm. The nadir pixel size for the longer UV (> 310 nm) and visible wavelengths is ~12 km x

Table 2: OMI OMI Product Information divided into U.S. Core (no shading), ROSES (gray), KNMI products (green), and FMI product (orange), KNMI and U. S. Core (blue), KNMI and ROSES (pink).

Product	Estimated Accuracy/Precision	Validation papers
Radiance	3%	<i>Dobber et al. [2008]</i>
Total column O ₃ Aerosol Index	1.5% N/A	<i>Kroon et al. [2008a,b]; McPeters et al. [2008]</i>
O ₃ profile	10%	(in development)
Tropospheric column O ₃	5-13 DU 1s low bias 1-7 DU	<i>Schoeberl et al. [2008]</i>
Surface UVB	0-30%	<i>Tanskanen et al. [2006,2007]</i>
Cloud pressure (optical centroid)	50 hPa	<i>Sneep et al. [2008]; Vasilkov et al. [2008]</i>
Aerosol optical extinction thickness	larger of 20% or 0.1 (cloud contamination)	<i>Curier et al. [2008]; Torres et al. [2007]</i>
Aerosol SSA	0.05	<i>Torres et al. [2007]</i>
SO ₂ column	anthrop.: 1-2DU 1s volcanic: 0.5 DU 1s biases: +/- 0.5 DU	<i>Krotkov et al. [2006;2008]; Yang et al. [2007]</i>
NO ₂ column	20% total column 50% trop. column	<i>Boersma et al. [2008a,b]; Bucsela et al. [2008]; Celarier et al. [2008]</i>
HCHO column	25-100% 1s	(in development)
BrO column	25-100% 1s	
OCIO slant column	25-100% 1s	

24 km, the smallest of any similar space-borne instrument. The swath is broad enough to provide global coverage in one day. OMI main data products are shown in **Table 2**. The Table shows that many of the OMI products are produced jointly by KNMI, FMI and the NASA OMI team.

OMI has been radiometrically stable as evidenced by the throughput changes (measured counts per unit radiance) which over the past ~5 years are of the order of few percent. However, there have been changes outside the instrument that affect the quality of OMI products. Although these changes are not considered life limiting, correcting for them will require a sustained effort throughout the mission lifetime, as discussed in Section 5. More information on the condition of OMI is provided in Section 7.3.3.

2.3 Tropospheric Emission Spectrometer (TES)

TES is a high-resolution infrared-imaging Fourier transform spectrometer with spectral coverage of 3.2-15.4 μm at a spectral resolution of 0.1 cm⁻¹, thus offering line-width-limited discrimination of a wide range of radiatively active molecular species in the Earth's lower atmosphere. The higher spectral resolution of TES compared to, for example, AIRS, allows the extraction of more tropospheric profile information on target trace gases. The main TES data are shown in **Table 3** [Beer, 2006; Beer et al., 2001]. TES is primarily nadir viewing, but can also observe the atmosphere in limb mode. In the nadir mode, TES has a spatial resolution of 0.53 x 5.3 km, but combines radiance spectra operationally to a swath size of 5.3 x 8.5 km. TES

provides day-night coverage and makes contiguous global measurements for 16 orbits (termed a global survey) every other day, alternating with opportunities for special observations. The TES data users guide and validation report can be found at <http://tes.jpl.nasa.gov/documents>.

Although the TES instrument has demonstrated increased component wear in the interferometer control subsystem (ICS), a performance risk item since pre-launch, it is in good health. There have been no hardware or software anomalies posing an immediate danger to the instrument. Periods of increased current draw in May 2005 and June 2008 led to modifications of TES operations in order to preserve instrument life, including elimination of the limb mode from routine operations after May 2005. The condition of the ICS is discussed in Section 7. Engineering data are available in Appendix E. With the present operational modifications in place, presuming all other systems continue nominal operations, TES should continue operations past 2011. More information on the condition of TES is provided in Section 7.3.4.

2.4 High Resolution Dynamics Limb Sounder (HIRDLS)

HIRDLS is a limb-scanning infrared filter radiometer with 21 channels between 6 and 17 microns designed to obtain profiles with 1 km vertical resolution of temperature, 10 atmospheric species important for ozone chemistry and Earth's radiative balance, as well as cloud types, cloud top heights, and aerosol extinction. HIRDLS, described by *Gille and Barnett [1992]* and *Gille et al. [1994; 1996; 2003]* is a joint development with the U.K., funded by the National Environment Research Council (NERC).

HIRDLS capabilities were compromised at launch when a piece of plastic film in the instrument came loose and blocked much of the aperture, allowing only a partial view at an azimuth angle of 47° from the orbit plane on the side away from the sun. The blockage precludes observations at multiple longitudes between orbit tracks, and limits geographical coverage to 65° S to 82° N. The obstruction necessitated substantial development of algorithms to remove effects due to the blockage and recover the atmospheric radiances. This unanticipated algorithm developmental effort delayed data delivery. *Gille et al. [2008]* describe an interim set of algorithms that allow species with larger radiometric signals to be recovered. Further efforts will be needed to improve the accuracy of the correction algorithms to recover of species with smaller signals, as described in Section 5.4.

The first set of data (V003), including temperature, O₃, HNO₃ and cloud top pressure was released in October 2007. Subsequent improvements led to V004 and additional constituents CFCl₃, CF₂Cl₂, and cloud and aerosol extinction. V004 was released in August 2008 and is now available from the Goddard DISC. These data sets are described in **Table 4**. Validation papers used V003 data. A discussion of V004 data and the updated validation results are contained in the HIRDLS Data Quality Document that is available from the DISC, or from the HIRDLS web site <http://www.eos.ucar.edu/hirdls/>.

HIRDLS is not currently collecting science data due to a chopper anomaly that began intermittently in early 2008.

Table 3: TES Core Product Information

Product	Useful Range	Estimated Precision & Accuracy	Vert. Res.	Validation papers
Level 1B Radiances	N/A	290-295 K: Bias <0.3K and σ <0.3K. 265-270K: Bias <0.5 K, and σ ~0.5K	N/A	Shephard et al. [2008a]
Temp.	10-1000 hPa	bias <0.6 K in lower trop, <0.5 K in upper trop and strat.; RMS 1.5 K in lower trop, 1 K in upper trop. and strat.	1 km in lower trop; ~3km above & limb	Herman et al. [2009] (in prep)
O ₃	10-1000 hPa (nadir) 10-300 hPa (limb)	Nadir: 3-10 ppb high bias in trop.; 7-16 ppb upper limit Limb: Low bias of 10-15% in lower strat High bias of 15-35% in upper strat. 15-30% RMS in strat.	4-6 km nadir 13-3 km limb	Worden H.M. et al. [2007]; Nassar et al. [2008]; Richards et al. [2008]; Osterman et al. [2008]; others in prep.
CO	100-1000 hPa	5-10% global averaged low bias; 15-20% RMS	6 km nadir	Luo et al., 2007a,b; Lopez et al., 2008
H ₂ O	200-1000 hPa	Nadir: Lower troposphere (moist): Bias: <5%, σ ~20 %; Upper trop. dry bias: ~15%, σ ~40%	2-4 km nadir 3 km limb	Shephard et al., 2008b
HDO	400-900 hPa	HDO/H ₂ O biased 5% high; expected precision: 1.5%	6 km	Worden J. et al., 2006
CH ₄	100-700 hPa	3-4% high bias; 1-2% 1 σ	8-9 km	Payne et al., 2008
HNO ₃	10-200 hPa	30% RMS	4 km	Coffey et al., 2008
Sea Surf. Temp.	N/A	0.15-0.3K low bias (night) ;0.2-0.4K low bias (day); 0.5-0.8 K 1 σ	N/A	Lampel, in prep
Cloud-top Pres.	N/A	30-200 hPa 1 σ , bias 50 hPa	N/A	Eldering et al., 2008
Cloud eff. τ	20-900 hPa	limited sens. at optical depths less than 0.2	N/A	Eldering et al., 2008

The chopper then stalled on March 17, 2008. All other subsystems are nominal. The team is continuing a plan to attempt chopper restart as described in Section. 7.3.1.

3.0 AURA PRIME MISSION ACCOMPLISHMENTS

The following sections summarize many of Aura’s scientific achievements. We emphasize those achievements that are directly related to the pre-launch Aura goals. We also include results of investigations that demonstrate the broader scope of scientific inquiry realized after launch. A complete listing of Aura publications is found at <http://aura.gsfc.nasa.gov/science/publications.html>. **Table 5** shows the relationship between the Aura science questions and the instrument measurements and highlights the multi-instrument synergy for addressing the questions.

3.1 Is the Ozone Layer Changing as Expected?

Complete ozone layer ‘recovery’ will be a slow process, detection of which will be complicated by climate change

and variability in atmospheric dynamics. Aura observations of ozone, ozone-destroying radicals, reservoirs of species affecting ozone, and long-lived trace gases, are a unique and essential resource for quantifying the complex interplay of dynamical, radiative and chemical processes that impact ozone recovery. As described in Section 4, extended Aura measurements are essential, not only for continuing needed long-term composition records, but also for validating our quantitative understanding of the middle atmosphere.

3.1.1 Trends in Stratospheric Trace Gases

Congressional Mandate and Clean Air Act requirements (1975, 1990) state that NASA is to monitor the state of the stratospheric ozone layer and atmospheric chlorine. OMI measurements of column ozone combined with MLS and HIRDLS ozone profile measurements along with other Aura measurements have allowed us to fulfill this requirement (**Figure 4** and **Figure 5**). The OMI column ozone measurements allow us to extend the total (column) O₃

Table 4: HIRDLS Core Product Information

Product	Useful Range	Estimated Accuracy	Vertical Res.	Validation papers
Temperature	1-400 hPa	± 0.5 K (cf sondes) 400-10 hPa ± 1 K (cf ECMWF) (to 1hPa)	1 km	Gille et al. [2008]
O ₃	1-260 hPa a	1 – 10% (5-200hPa) 5 – 20% (200-260hPa)	1 km	Nardi et al. [2008]
HNO ₃	10-161 hPab	10-15%	1 km c	Kinnison et al. [2008]
CFCl ₃	26.1-287.3 hPa	~30% (for zonal mean)	1-1.2 km	In preparation
CF ₂ Cl ₂	10.0-287.3 hPa	~30% (for zonal mean)	1-1.2 km	In preparation
Cloud top pressure	10-422 hPa	± 20%	1 km	Massie et al. [2007]
Cloud and aerosols extinction	20-215 hPa	Use extinction between 10-5-10-2 km-1. Precision in 0-100% range.	1 km	In preparation

a. In the tropics there is a high bias of ~50% at 70 hPa and a high bias >150% at 100 hPa.
b. Depends on latitude.

c. Varies with latitude and altitude.
d. Use extinction in a qualitative manner.

record initiated by Nimbus 7 TOMS in 1978. Total O₃ is obtained from OMI using the TOMS Version 8 algorithm [Bhartia and Wellemeyer, 2002] and is included in the climate data record (CDR). The OMI data provide additional information from a stable orbit, adding confidence to the record. The merged O₃ CDR, including SBUV, TOMS and OMI data, was used in analysis of total O₃ changes reported in WMO [2006] (Figure 4).

International treaties now ban production of manmade chlorofluorocarbons (CFCs). CFCs are the primary source of stratospheric chlorine and HCl is the primary chlorine reservoir in the upper stratosphere. Measurements of upper stratospheric HCl thus provide a quantitative assessment of total atmospheric chlorine. HCl measurements from MLS link to the record of stratospheric HCl measurements by HALOE aboard UARS begun in 1991. The HALOE measurements were terminated after about one year of overlap with Aura MLS so we now have a good combined record of stratospheric chlorine. Near the stratopause MLS HCl has begun to decrease in accord with expectations based on ground-based measurements of source gases [Lary et al., 2007; Froidevaux et al., 2006; Lary and Aulov, 2008]. Although the primary MLS band used to measure HCl is operated only sparingly due to the limited lifetime of a failing component, periodic observations of upper-stratospheric HCl trends will continue (as described later). Additionally, measurements of HCl in an adjacent band (Figure 5) provide information concerning the HCl morphology and chlorine partitioning in the lower and middle stratosphere.

3.1.2 Ozone Hole Photochemistry

Aura has revealed important new details about the Antarctic O₃ hole and Arctic ozone loss including the timing of the transformation of trace gases HNO₃, HCl and ClO as the vortex temperature declines and the dramatic rapid re-appearance of HCl once all the ozone is depleted [Santee et al., 2005; Manney et al., 2005]. The northern winter stratospheric vortex is far more seasonally variable and more subject to injections of air from lower latitudes [Schoeberl et al., 2006a; Leblanc et al., 2006]. Nonetheless

Table 5: Linkage between Aura instrument measurements and science questions.

Science Questions	Instrument	Measurement
Is the ozone layer changing as expected?	MLS	O ₃ , HNO ₃ , N ₂ O, H ₂ O, ClO, HCl, CO OH, HO ₂ , HOCl, BrO, Temperature
	HIRDLS	O ₃ , HNO ₃ , H ₂ O, CH ₄ , CFC11, CFC12, Volcanic aerosols, Stratospheric Clouds, Temperature
	OMI	Column Ozone, O ₃ Profile
What are the processes that control tropospheric pollution?	MLS	CO, O ₃ , Temperature
	OMI	NO ₂ , SO ₂ , HCOH, Column O ₃ , Aerosols
	TES	CO, O ₃ , HDO, Temperature
What are the roles of upper tropospheric aerosols, water vapor, and ozone in climate change?	MLS	Cloud Ice, H ₂ O, O ₃ , Temperature
	HIRDLS	O ₃ , H ₂ O, Volcanic aerosols, Cloud height, Cirrus
	OMI	O ₃ , Aerosols, Cloud pressure
	TES	O ₃ , H ₂ O, HDO, CH ₄ , Temperature, Cloud pressure

with the excellent north polar coverage provided by Aura, we have been able to quantify chemical O₃ loss [Singleton et al., 2007; Manney et al., 2006a; El Amraoui et al., 2008; Rösevall et al., 2008; Jackson and Orsolini, 2008].

Key to initiating polar ozone loss is the formation of polar stratospheric clouds (PSCs). These clouds form in the cold winter stratosphere and are composed of HNO₃ hydrates and water vapor. Chemical reactions on PSC surfaces convert HCl and ClONO₂ into Cl₂ and HNO₃ which begins catalytic ozone destruction. HIRDLS observations of the distribution of northern hemisphere PSCs complement measurements made by CALIPSO. MLS and HIRDLS observations of the changes in HNO₃ and H₂O during the formation of the ozone hole have been used to investigate dehydration through sedimentation of PSC particles within the polar vortex [Jiménez et al., 2006]. The denitrification of the vortex (HNO₃ removal) is a key process which allows the ozone catalytic cycle to take place. Unless HNO₃ is removed, it can photolyze producing NO₂ that will combine with ClO forming ClONO₂ halting the catalytic cycle.

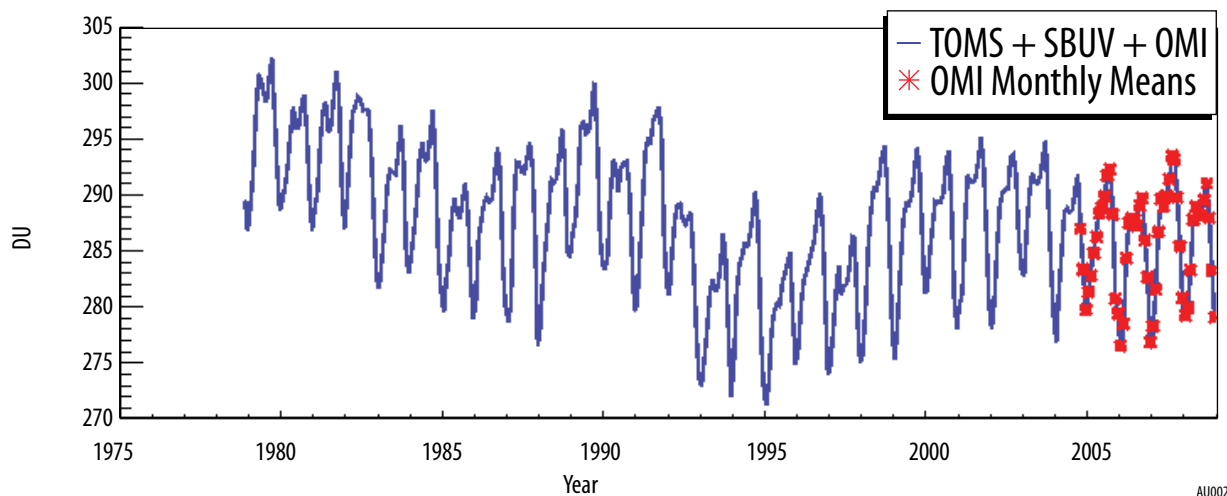


Figure 4: 60°S–60°N total column O₃ merged TOMS/SBUV/OMI data set.

Most recently *Pope et al.* [2007] made new laboratory measurements of the chlorine dimer (Cl_2O_2) photolysis rate arriving at a lower number than previously measured. **Figure 6** compares observations, a simulation using standard values for photolysis of Cl_2O_2 and a simulation using *Pope et al.* values. It is clear from the figure that the *Pope et al.* rates cannot account for the amount of ClO observed by MLS. In short, we have a wealth of observations in polar regions clearly demonstrating chlorine activation and ozone depletion. Those observations cannot be reconciled with our current understanding of chemical ozone loss mechanisms if the *Pope et al.* parameters are utilized in models. Continued observations, modeling and laboratory work are required to resolve this dilemma.

In summary, Aura data have been used to test and constrain the physics in models of cloud and ice formation and to test the bromine and chlorine chemistry, including the possibility of a much slower dimer photolysis than the standard value. High resolution observations of temperature and traces species are being used to evaluate transport pathways and mixing processes that are critical to the ozone budget in the climatically important UTLS region. Aura



Figure 5: HCl abundance near 55 km 1985 - present. The Aura MLS Band 13 HCl observations (red dots) are more reliable for trend studies than the continuous Band 14 record (red crosses) although Band 13 data are intermittent after 2006 as discussed in the technical section 7.3.2. Also shown are model predictions using a mean age value of 5.5 years and spectrum widths of 0 years (blue) 2 years (black) and 4 years (orange). The biases between the measurements are within the accuracy of the instruments.

data are being assimilated in models to evaluate chemical and dynamical processes. These studies have revealed model areas in need of improvement, and will lead to better understanding of physical, chemical and dynamical processes. The net result will be more credible assessments of the future evolution of the stratospheric ozone layer.

3.1.3 Ozone Photochemistry and Middle and Low Latitude Ozone Depletion

Although less dramatic, ozone changes outside the polar regions have more environmental impact than polar ozone depletion. Uncertainty still exists in explaining these changes and the role of short lived chlorine compounds in the chlorine budget as well as the importance of bromine. *Livesey et al.* [2006] use MLS BrO measurements to estimate a contribution (3 pptv) from very short-lived halogenated species to the uncertain stratospheric bromine budget. MLS data are also used to characterize regions of O_3 -poor air that are common in Aleutian and Australian anticyclones during northern hemisphere winter and southern hemisphere spring. These regions are produced by a combination of chemical and dynamical processes [*Harvey et al.*, 2008].

The role of the hydroxyl radical chemical processes that control upper stratospheric ozone has been controversial since the 1990's when MAHRSI measurements produced OH profiles at odds with stratospheric models. One of the goals of the MLS THz radiometer was to make improved OH measurements in the stratosphere and mesosphere. Within the first year of launch, MLS OH and HO_2 data were found to be consistent with models and laboratory photochemical reactions used therein [*Pickett et al.*, 2006a; *Canty et al.*, 2006], refuting the existence of the so-called "HO_x dilemma". MLS OH data have also revealed details about O_3 and OH photochemistry and their link to solar activity. *Pickett et al.* [2006b] confirm a nighttime layer of OH near 82 km in the mesosphere, previously observed by ground-based lidar. MLS observes increases in mesospheric OH (and associated decreases in O_3) during/after solar proton events (SPEs). Variations in MLS O_3 and temperature in the lower stratospheric tropics and at high latitudes in winter follow the 27-day variations in solar UV radiation [*Ruzmaikin et al.*, 2007].

HIRDLS delivered validated data to the scientific community much later than other Aura instruments due to the required re-build of the retrieval algorithm. Even so, the high vertical resolution of HIRDLS data provide exciting new insights into transport processes within the stratosphere. *Nardi et al.* [2008] demonstrated that layered features seen in HIRDLS ozone agree with observations from ozonesondes (**Figure 7**) and these layers also exist in the HNO_3 observations [*Kinnison et al.*, 2008]. *Olsen et al.* [2008] showed that these layers are coherent and can be followed from the tropics to middle and high latitudes. The NASA Global Model Initiative (GMI) 3D CTM produces structures similar to those observed by HIRDLS validating their generation by the model. *Yudin et al.* [2009a] used HIRDLS data and model simulations to show that these laminae occur most frequently during March-April in the Northern Hemisphere, but are much less frequent in the Southern Hemisphere.

Although Aura does not measure winds directly, observations of long-lived tracers and temperature also provide information about transport processes in the upper atmosphere. *Manney et al.* [2008a; 2008b] used O₃, temperature and N₂O measurements to characterize the evolution of the stratopause and stratospheric vortex during major sudden warmings. *Feng et al.* [2007] detect slow equatorial Kelvin waves in temperature and O₃. *Manney et al.* [2006b] describe an unusual event during which a region of high values of a long-lived tracer is drawn into the Aleutian anticyclone at the end of the 2005 northern winter. Because of the timing of this event, the region of high values persisted for months following the transition to the summer circulation.

The overall chemical transport circulation of the stratosphere is driven, in part, by breaking gravity waves which are parameterized in models. However, Aura MLS measurements give us the information about global gravity wave variance [*Wu and Eckermann, 2008*], and the high vertical resolution profiles from HIRDLS give us the first real clue about the magnitude of gravity wave momentum fluxes [*Alexander et al., 2008; Wright et al., 2009*].

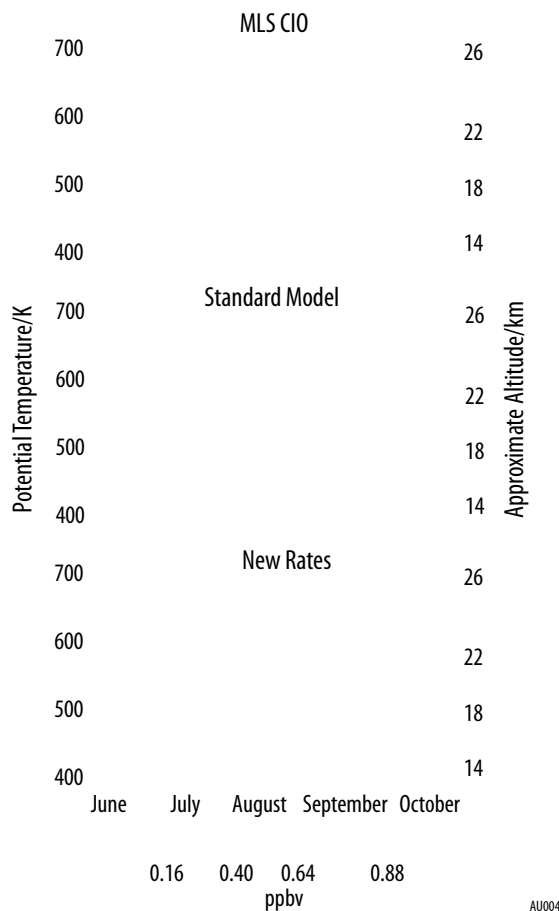


Figure 6: Vortex averaged MLS ClO for the 2005 Antarctic winter/spring (top) agrees well with a SLIMCAT simulation using the standard input to calculate ClO dimer photolysis (Standard model). The bottom simulation uses recent *Pope et al.* [2007] laboratory results for dimer photolysis. This simulation differs markedly from MLS observations (i.e., enhanced ClO). Adapted from *Santee et al.* [2008a].

3.1.4 Summary

‘Recovery’ in the stratospheric ozone layer will be a slow process, discernment of which (including the impact of climate change) will be complicated by concurrent variability in atmospheric dynamics and meteorology. Aura observations of ozone, along with source gases, radicals and reservoirs of species affecting ozone, and long-lived dynamical tracers, are a unique and essential resource for quantifying the complex interplay of dynamics, radiation and chemistry that control ozone layer stability. As described in Section 4, extended Aura measurements are essential, not only for continuing needed long-term composition records, but also for validating our quantitative understanding of the middle atmosphere and its response to changes in halogen loading and climate.

3.2 What are the Processes that Control Tropospheric Pollutants?

Until the launch of Aura, there has been no consistent global assessment of air quality with the coverage that remote sensing can provide. Aura is unique in that it can measure all of the EPA criteria pollutants (except lead) and even some of the volatile organics that contribute

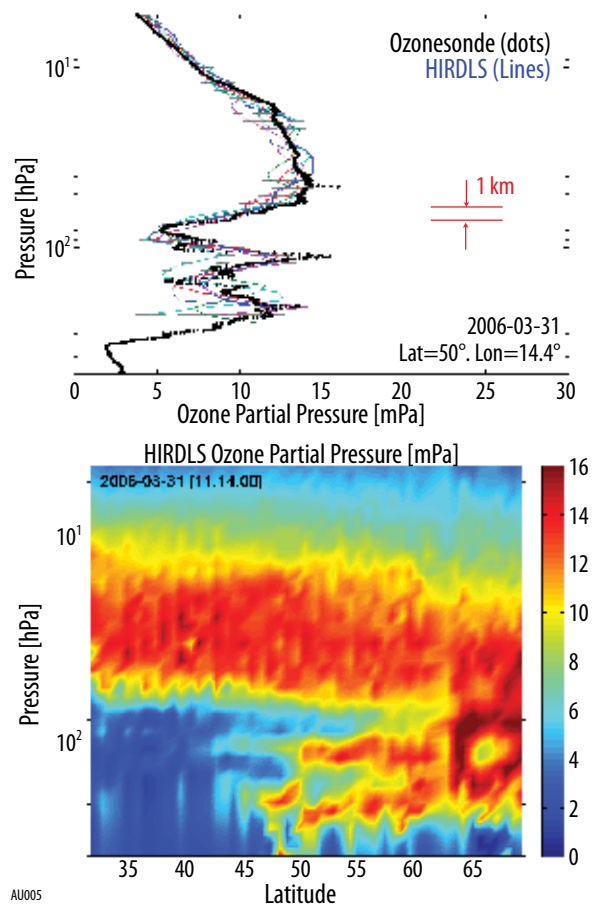


Figure 7: (top) Comparison between an ozonesonde and the closest eight coincident HIRDLS, indicates the vertical features captured by HIRDLS. (bottom) Curtain plot of O₃ partial pressure along a scan track through the location of the sounding [*Nardi et al., 2009*].

to smog. The criteria pollutants are sulfur dioxide (SO₂), nitrogen dioxide (NO₂), carbon monoxide (CO), tropospheric O₃, and aerosols. OMI also retrieves information about formaldehyde (HCHO) and glyoxal (CHO-CHO), both volatile organic compounds (VOCs), and TES has now demonstrated the capability to measure high concentrations of ammonia (NH₃), a key aerosol precursor, and methanol (CH₃OH), another VOC. VOCs, CO, and NO₂ are tropospheric O₃ precursors, and NO₂, HCHO and SO₂ contribute to the formation of aerosols. There are also strong linkages between these constituents and climate. For example, the El Niño affects distributions of pollutants because it changes the pattern of biomass burning and the wind fields responsible for long range transport. Tropospheric O₃ and aerosols impact climate through their effects on the radiation budget. These linkages are detailed further in Section 3.2.3. Complementary measurements from TES, MLS, and OMI and other sensors are being used to untangle the complex interaction between emissions, chemistry, physical processes, and dynamics that contribute to tropospheric composition and air quality as described below.

3.2.1 Sulfur Dioxide (SO₂) from OMI and TES

How much sulfur dioxide is generated naturally and how much is generated by man-made processes? Volcanoes (both erupting and fuming) are a principal source of natural SO₂, and volcanic ash plumes are a hazard for aviation. Accurate inventories of man-made SO₂ sources (mostly smelters and coal burning power plants) outside the first world countries are not available. OMI measurements have changed this picture. For example, OMI can clearly see the SO₂ being emitted from the La Oroya and Ilo copper smelters in Peru even though these produce less SO₂ than the nearby volcanoes in Ecuador [Carn *et al.*, 2007b]. Comparisons of current models with OMI data suggest important biases in previous anthropogenic SO₂ emission inventories [Lee *et al.*, 2009].

Observing volcanic plumes and their evolution is an important application for aviation, and in addition allows us to test transport models. Carn *et al.* [2009], using daily, global OMI measurements found that some volcanic clouds tend to occupy the jet stream, suggesting an increased threat to aircraft. The volcanic cloud from the May 2006 eruption of Soufriere Hills Montserrat was tracked by OMI for over three weeks as it drifted westward in the tropical lower stratosphere. This cloud was also detected by CALIPSO in its 'first light' measurements in June 2006 [Carn *et al.*, 2007a]. Prata *et al.* [2007] used TES IR as well as OMI UV SO₂ observations to study the Soufriere Hills plume.

OMI is useful for monitoring daily SO₂ emissions from hazardous volcanoes. Sawyer *et al.* [2008] used OMI SO₂ and ground-based DOAS measurements from Nyiragongo to show that volcanic degassing rates derived from OMI SO₂ are consistent with rates from established monitoring techniques. Clerbaux *et al.* [2008] retrieved SO₂ vertical profiles within volcanic plumes with TES, providing information on both the quantity of gas emitted and its altitude. Elevated SO₂ total columns retrieved with TES following volcanic eruptions in 2005 are in good agree-

ment with those from OMI. Carn *et al.* [2008] used OMI data to extract daily SO₂ burdens and information on SO₂ sources for active volcanoes in South America between 2004 and 2006, showing that OMI distinguishes SO₂ from multiple emitting sources. OMI detected variations in SO₂ release related to cycles of volcanic conduit sealing and degassing. Information from OMI and Aqua AIRS (with its broader swath) can be combined to obtain the volcanic cloud altitude.

3.2.2 Nitrogen Dioxide (NO₂) from OMI

Nitric oxide (NO) is formed by lightning and biomass burning as well as combustion processes associated with power plants and internal combustion engines. NO₂ is then created from the reaction of NO with ozone or other oxidizers. NO₂ has a short lifetime and is usually concentrated near its sources. The high spatial resolution of OMI NO₂ data provide a new and dramatic view of the planet, allowing us to constrain emission inventories and showing us the location of potential ground level ozone formation, isolated emission sites and even high automobile and truck traffic regions. For example, Wang *et al.* [2007] showed evidence of reductions in NO₂ based on OMI data associated with traffic restrictions put in place in China. Boersma *et al.* [2009] (using OMI and SCIAMACHY data) found that the diurnal cycle in NO₂ in OMI data over Israeli cities is weaker in winter than summer due to strongly reduced photochemistry, and Zhang *et al.* [2008] used OMI data to constrain emission estimates of NO_x in eastern Asia, helping to explain the high ozone concentrations measured over the Pacific Ocean during the 2006 INTEX-B campaign. Boersma *et al.* [2008b], also attempting to constrain emission estimates, found reductions of industrial NO_x emissions and increases in vehicular emissions over the U.S. and soil emissions over Mexico. Work in progress by the OMI and TES teams relates NO₂ and VOC concentrations to ozone production. OMI is the first instrument in space capable of measuring NO₂ in near-real-time (NRT) on a day-to-day basis Boersma *et al.* [2007].

3.2.3 Carbon Monoxide (CO) from MLS and TES

One of the most dramatic discoveries emerging from the MLS data is the high concentration of CO localized over the Tibetan plateau during summer. High surface CO concentrations are apparently being drawn up through the cyclonic monsoon circulation emerging in the anti-cyclonic circulation in the lower stratosphere [Filipiak *et al.*, 2005; Li *et al.*, 2005a]. This massive rapid uplift appears to short circuit the normal slower uplift characteristic of the tropical upper tropospheric layer [Fu *et al.*, 2005; Park *et al.*, 2007; James *et al.*, 2008] where variations in MLS CO are due more to the seasonal variation in convective transport rather than in surface CO emissions [Jiang *et al.*, 2007].

Upper tropospheric and lower stratospheric measurements of CO from MLS complement the tropospheric information obtained from TES. Assimilated MLS CO observations have been used to diagnose transport of African pollution [Barret *et al.*, 2008] and assimilated TES CO to investigate near real-time biomass burning estimates [Al-

Saadi et al., 2008]. Jones et al. [2007] assimilated TES CO measurements and found that continental emissions in the southern hemisphere were 2-3 times higher than climatological estimates. These high regional emissions increased free tropospheric O₃ by 10-15 ppb, as observed by TES over Indonesia/Australia [Bowman et al., 2008].

3.2.4 Tropospheric O₃ and VOCs from TES, OMI, and MLS

Remote sensing of tropospheric O₃ from space is difficult, because approximately 90% of the total column resides in the stratosphere. Aura sensors have provided the most accurate remote sensing estimates of tropospheric O₃ to date, including regions outside the tropics. TES tropospheric ozone profile measurements have a vertical resolution of approximately 6 km. This vertical resolution is sufficient to resolve the lower troposphere from the upper troposphere for tropical clear sky conditions and produce an average tropospheric column at polar latitudes, depending on cloud conditions.

The Tropospheric O₃ Residual (TOR) is the difference between the observed total column O₃ and a co-located stratospheric O₃ column and therefore provides an estimate of the total tropospheric column at OMI spatial resolution. Ziemke et al. [2006] applied this technique using OMI and MLS, comparing results to a simulation from a chemistry and transport model (CTM). Stajner et al. [2008] assimilated OMI and MLS data to produce a TOR. Jing et al. [2006] showed good agreement between a similar TOR product and sonde data. Schoeberl et al. [2007] used trajectory mapping of MLS observations to produce a high horizontal resolution daily stratospheric column roughly matching the OMI spatial resolution. They showed that the TOR was highly correlated with ozonesonde tropospheric ozone columns and TES com-

puted TOR. Accuracy of their product was further improved in cloudy pixels using OMI-derived optical centroid cloud pressures [Joiner et al., 2009a]. **Figure 8** shows the 2007 summer residual column computed using the method of Schoeberl et al. Visible in the figure are the pollution build up and transport from China into the Pacific, from eastern United States and Europe into the North Atlantic, from biomass burning regions in Africa into the South Atlantic and South Pacific, and from the western United States into the Pacific.

Ziemke et al. [2009] employed a cloud-slicing approach with OMI and MLS O₃ and OMI cloud retrievals to derive O₃ mixing ratios within the top portions of deep convective clouds and showed that tropical Pacific clouds, drawing ozone depleted air from the boundary layer, have almost no ozone within them. TOR has also been used in studies of pollution transport [Duncan et al., 2008; 2007] and seasonal and interannual variations in O₃ distribution [Choi et al., 2008; Chandra et al., 2007; Ziemke et al., 2007]. Martin et al. [2007] used TOR with data from other satellite instruments to estimate the global annual budget of NO_x from lightning: -6 Tg N/yr.

The vertical information and tropospheric sensitivity provided by TES ozone measurements allow insights that cannot be gained from other ozone products or other sensors with lower spectral resolution (such as AIRS or IASI).

TES revealed different vertical distributions for tropospheric O₃ south and north of the ITCZ over the tropical Atlantic Ocean during the North African biomass-burning season [Jourdain et al., 2007] (**Figure 9**). Liu et al. [2009] used O₃ and CO profiles from TES, along with the GEOS-CHEM CTM, to show that the Asian monsoon lofts and transports O₃ and its precursors to the Middle East, impacting the O₃ distribution in this region. This analysis also

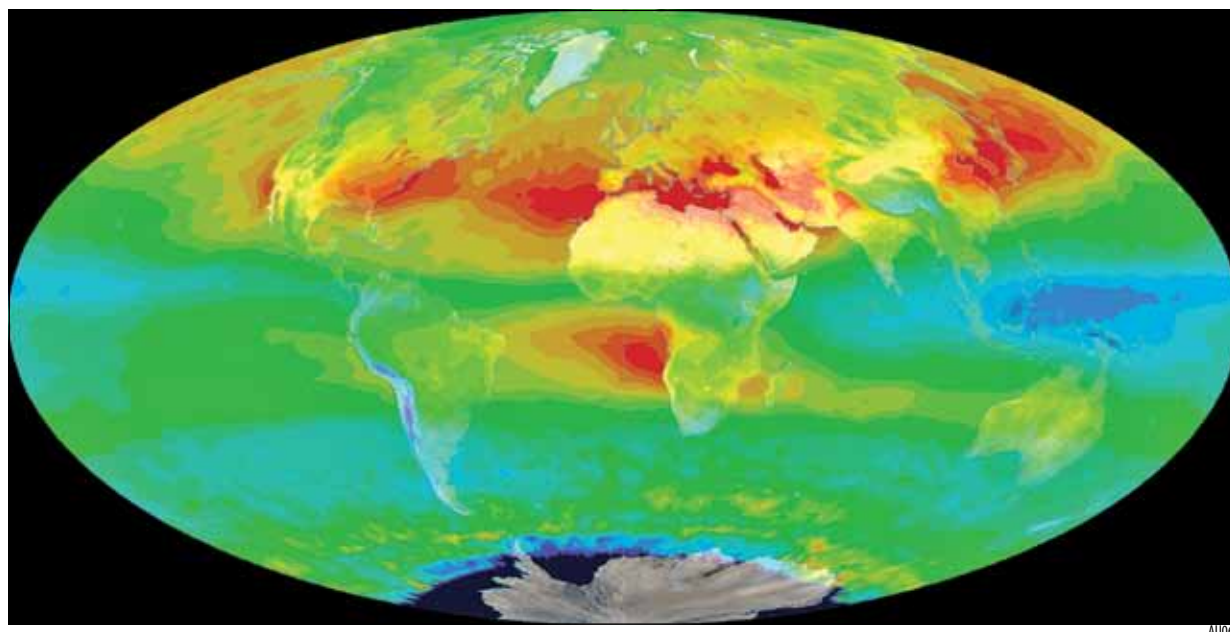


Figure 8: Tropospheric ozone residual for June-August 2007 computed by subtracting the MLS stratospheric column from the OMI total column described by Schoeberl et al. [2007]. Colors range from dark blue to red indicate 0-40 Dobson Units.

used TES water vapor isotope measurements to identify the moisture transport characteristics of the summertime monsoons, as air parcels from Africa and Asia have different water isotopic signatures. *Verma et al.* [2009], using TES O₃ and CO along with OMI aerosol optical depth and NO₂, found enhanced O₃ levels near and away from Siberian forest fires when sunlight and NO_x are available.

Logan et al. [2008] showed large differences in TES CO, O₃, and H₂O over Indonesia and the eastern Indian Ocean in October – December 2006 relative to 2005. These differences were due to the low rainfall and changing convection patterns due to El Niño. Drier air also leads to more biomass burning and higher fire emissions (marked by higher CO) in 2006. *Chandra et al.* [2009] also investigated the effects of El Niño using OMI and MLS data to show that the global burden of CO increased by 8-12% while the global O₃ burden increased by 2-3% during the moderate 2006 El Niño event. *Sauvage et al.* [2007] used OMI, MLS, and *in situ* observations to show that the tropical lightning source of O₃ is ~4-6 times greater than that from biomass burning, soils, and fossil fuels. The distributions of tropospheric constituents are correlated with the Madden Julian Oscillation (MJO) as seen in MLS CO, cloud and H₂O observations [*Schwartz et al.*, 2008; *Wong and Dessler*, 2007].

Zhang et al. [2006; 2008] exploit the vertically resolved O₃ and CO measurements from TES to identify the influence of polluted continents on downwind air quality, and the later study concluded that Asian pollution enhanced surface ozone concentrations by 5–7 ppbv over western North America in spring 2006. *Millet et al.* [2008] used OMI HCHO to show that emissions from the dominant isoprene source regions are overestimated (by as much as 70%) in the standard emission inventories, an important result for air quality since isoprene is a precursor of ground-level O₃ and fine particulate matter (PM). *Duncan et al.* [2009] found that drought, surface O₃, and temperature contribute to the variability in isoprene emissions and thus variability in HCHO columns measured by OMI in the southeast US for 2005-2007.

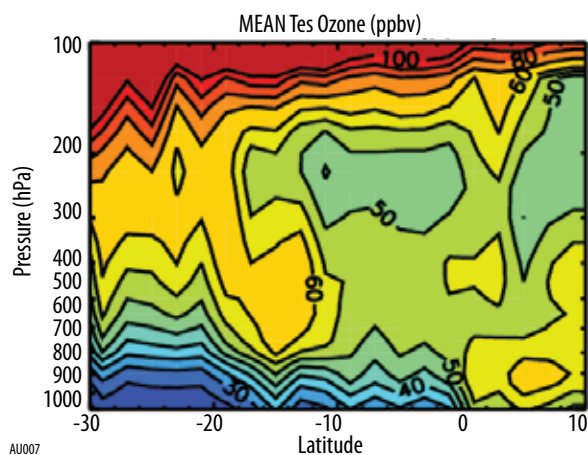


Figure 9: Vertical distribution of TES ozone over the Atlantic corridor corresponding to January 22-25, 2005 TES special observations. Zonal average from -30°E to 10°E includes 416 ozone profiles.

TES observations are now being assimilated in a number of models. For example, using data assimilation techniques, *Parrington et al.* [2008] constrained ozone predictions from GEOS-Chem and AM2-Chem during the summer of 2006 with TES observations. These models under-predicted mid-tropospheric ozone by as much as 40% and were corrected to within 5% of independent ozone-sonde measurements after assimilating the TES satellite measurements.

3.2.5 Summary of Processes that Control Tropospheric Pollutants

As a result of the extensive Aura measurements, processes controlling tropospheric pollution have been better quantified, such as the SO₂ emissions of volcanoes and smelters, NO_x emissions, and the global movement of CO, ozone, and water, and how that is impacted by the Asian Monsoon, El Niño, pollution outflow from continents, and regional pollution. To differentiate the role of a range of factors (dynamics, natural emissions, human emissions), measurements that sample a broader range of conditions are required. Section 4 describes more fully the conditions that need to be sampled and their relationship to the Aura science questions.

3.3 What are the Roles of Upper Tropospheric Aerosols, Cirrus Clouds, Water Vapor, and Ozone in Climate Change?

Trace gases, clouds and aerosols contribute to the radiative budget of the atmosphere. Aerosols also modify clouds through the indirect and semi-direct effects. The impact of aerosol and cloud feedbacks on the climate system has the greatest uncertainty of any climate forcing. Aura instruments provide unique measurements of trace gases, aerosols and high tropospheric clouds that compliment other measurements being made in the A-Train.

3.3.1 Clouds, H₂O, HDO and aerosols

The role of tropical cirrus in the radiative transfer budget of the planet has always been controversial. HIRDLS, MLS, OMI and other A-train sensors provide complementary information about these clouds. HIRDLS measures thin clouds in the upper troposphere and stratosphere that play an important role in the tropics, impacting the radiative balance and the amount of water vapor entering the stratosphere. MLS measures water vapor and trace gases in the presence of aerosol and all but the thickest clouds and can make measurements of the ice water content of thick clouds. A comprehensive climatology for occurrence of thin clouds from HIRDLS and back-scatter measurements from CALIPSO reveals detailed spatial-temporal structure of upper tropospheric clouds and water vapor and serves as a statistical test of cloud distributions and properties in climate models. (**Figure 10**).

MLS measures upper tropospheric water vapor in the presence of clouds, providing critical new information on climate feedbacks in the tropics. *Su et al.* [2006a,2008] quantified the relationship between MLS/AIRS cloud observations and SST, showing that upper tropospheric

clouds generally have a positive climate warming feedback, refuting the ‘iris hypothesis’ of Lindzen *et al.* [2001]. They also reported a sharp increase in MLS observations of upper tropospheric H₂O and cloud ice, indicative of deep convection, for sea surface temperatures (SST) greater than 300K. This upper tropospheric moistening can account for ~65% of the previously-reported ‘super greenhouse effect.’

The unanticipated measurement of HDO by TES has given us a completely new perspective on the hydrological cycle. The relative distribution of H₂O to HDO is sensitive to evaporation and condensation processes because HDO preferentially condenses relative to H₂O. Even paleo-records ice core show the imprint of preferential condensation of HDO [Noone, 2008]. TES measurements of H₂O and its isotopes (Figure 11) [Worden *J. et al.*, 2006; Worden *J. et al.*, 2007a] have been used to estimate the relative contributions of advection, convection, evaporation (source) and condensation (sink) strengths over tropical continents [Brown *et al.*, 2008]. TES measurements of the isotopic composition of water are now being used to estimate evaporation and precipitation strengths to understand how climate variations will affect precipitation patterns.

OMI-derived aerosol extinction optical thickness (AOT) and single-scattering albedo (SSA) of aerosols over arid land masses have comparable or better quality [Torres *et al.*, 2007; Ahn *et al.*, 2008] than multi-spectral/angle satellite visible/near IR retrievals. Although superior to heritage instruments, the typical pixel size of OMI (~1000 km²) is still

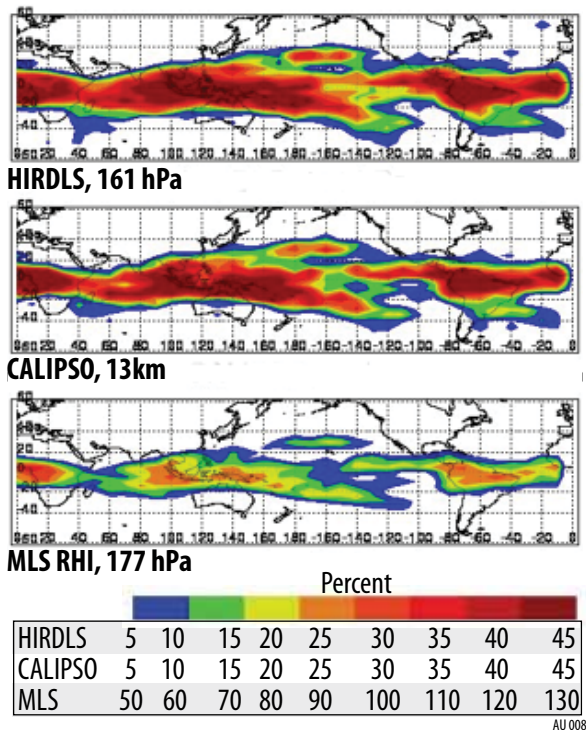


Figure 10: HIRDLS (top) and CALIPSO (middle) cloud frequency of occurrence at 161 hPa and 13 km altitude during April 2007 and MLS RHI (bottom) at 177 hPa [Massie *et al.*, 2009]

too coarse for accurate retrieval of AOT outside arid areas because of cloud contamination. However, aerosol absorption optical thickness (AAOT) can be estimated accurately even when a pixel is contaminated with clouds, snow, or ice. Figure 12 shows large changes in the AAOT over S. America during the biomass burning season that are consistent with MODIS fire count data and likely due to changes in land use [Torres *et al.*, 2009]. The multi-wavelength algorithm provides 2 to 4 degrees of freedom for characterizing aerosol properties [Veihelmann *et al.*, 2007] and is used to estimate the short-wave direct radiative forcing at the top of the atmosphere [Veihelmann *et al.*, 2008].

3.3.2 Chemistry and Climate

By design, Aura instruments stress the troposphere and lower stratosphere. Interactions between the troposphere and stratosphere are important to the stratospheric ozone layer through changes in stratospheric humidity and dynamics and to climate through changes in stratospheric O₃, radiative and dynamical influences of the stratosphere on the lower atmosphere, and transport of stratospheric air into the troposphere. Most transport of air from the troposphere to the stratosphere takes place in the tropics. The

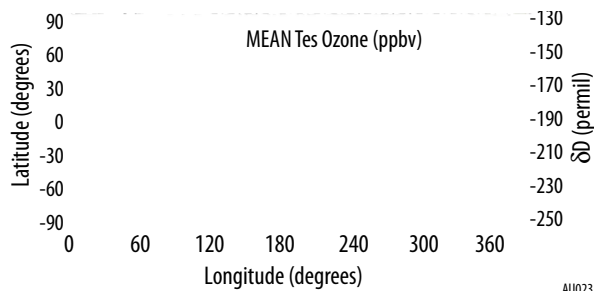


Figure 11: Global map of the lower tropospheric HDO/H₂O ratio in units of parts per thousand relative to the isotopic composition of ocean water.

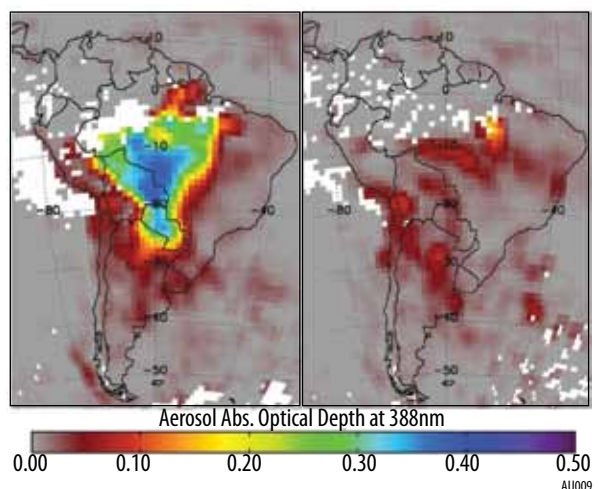


Figure 12: OMI-retrieved aerosol absorption optical depth at 388 nm for September 2007 (left) is much higher than September 2008 (right).

radiative balance of the atmosphere depends on the distributions of constituents like O₃ and H₂O and, through the constituent distributions, is coupled to the photochemical and transport processes.

Tropical Composition

The tropical tropopause layer (TTL) is the region between 15 km and 18 km where air is dehydrated as it ascends into the stratosphere. The air emerging from the TTL rises slowly through the lower stratosphere producing anomaly patterns. This is called the “tape recorder”. *Read et al.* [2008] show the complete vertical extent of the water vapor tape recorder and its relationship to overshooting convection to produce the observed signature. MLS data also show tape recorder signatures in CO [*Schoeberl et al.*, 2006b] and HCN [*Pumphrey et al.*, 2008] as shown in **Figure 13**. Seasonal changes in upwelling and convective outflow both contribute to the seasonal cycle in O₃ and CO [*Randel et al.*, 2007]. *Schoeberl et al.* [2008a] quantified the influence of both the Quasi-biennial Oscillation (QBO) and Brewer-Dobson circulation (BDC) on the abundance of a range of trace gases in the TTL and tropical lower stratosphere. *Schoeberl et al.* [2008b] were able to estimate the vertical velocity in the lower stratosphere using the tape recorder signal, showing it was consistent with radiative transfer estimates. Climate models show that this upwelling should slowly accelerate. A continued record of stratospheric observations is required to discern such subtle signatures.

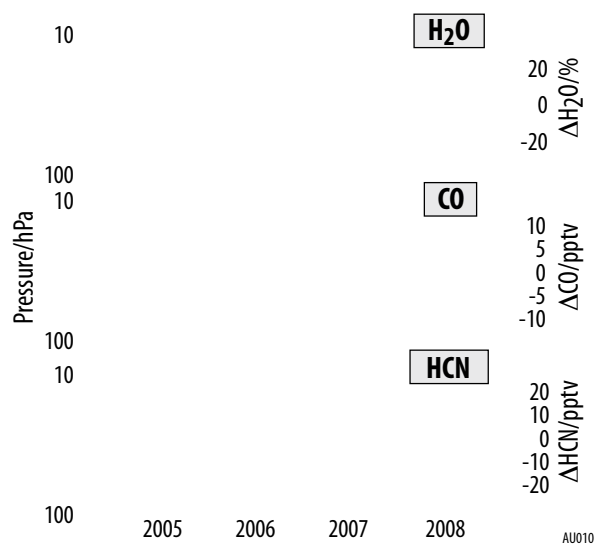


Figure 13: Timeseries for the departure of daily averaged MLS tropical profiles of H₂O, CO and HCN from the time mean profile exhibit the ‘tape recorder’ signature. Annual variations in the ‘cold point’ (~100 hPa) temperature control the amount of H₂O entering the tropical stratosphere, and alternating bands of wet and dry air slowly ascend. The seasonal cycle in pollution drives the annual variation in CO. The CO signature falls off with altitude due to chemical loss. The HCN signature extends to higher altitude than that of CO because HCN has a longer lifetime but appears to exhibit a two-year rather than a one-year cycle. A longer record is required to characterize this signature.

Radiative effects of Tropospheric O₃

Tropospheric O₃ absorbs sunlight and infrared radiation and is the third most important greenhouse gas [IPCC, 2008]. The IPCC’s estimate of the greenhouse contribution from ozone is also the most uncertain due to uncertainty in the horizontal and vertical ozone distribution. Until Aura measurements, estimates of the greenhouse contribution of ozone were only from models. *Worden et al.* [2008] calculated the instantaneous clear-sky greenhouse contribution from upper tropospheric O₃ from TES thermal radiances as shown in **Figure 14**. The globally averaged estimate from these clear-sky values is consistent with that used in the most recent IPCC; however, the observed horizontal and vertical distributions were found to be significantly different. *Joiner et al.* [2009a] computed both the long- and short-wave seasonal radiative effect of tropospheric O₃ in all-sky conditions using TOR and cloud data from OMI and MODIS, providing further tests for the IPCC models.

3.3.3 Summary

Aura discoveries have resulted in valuable advances in our understanding of climate, including quantification of cloud, water vapor and ozone radiative forcings and feedbacks, as well as new insights into atmospheric dynamics and the hydrological cycle. As will be described in Section 4, recent adjustments to the Aura orbit and the change in the MLS THz scan enable new Aura extended mission cloud observations, that complement those from CloudSat and CALIPSO. A longer record of Aura observations, encompassing a broad range of variability (such as El Niño’s, the Arctic Oscillation, and MJO), is essential for validating climate models and improving the predictability of future climate.

Aura discoveries have resulted in valuable advances in our understanding of climate, including quantification of cloud, water vapor and ozone radiative forcings and feedbacks, as well as new insights into atmospheric dynamics and the hydrological cycle. As will be described in Section 4, recent adjustments to the Aura orbit and the change in the MLS THz scan enable new Aura extended mission cloud observations, that complement those from CloudSat and CALIPSO. A longer record of Aura observations, en-

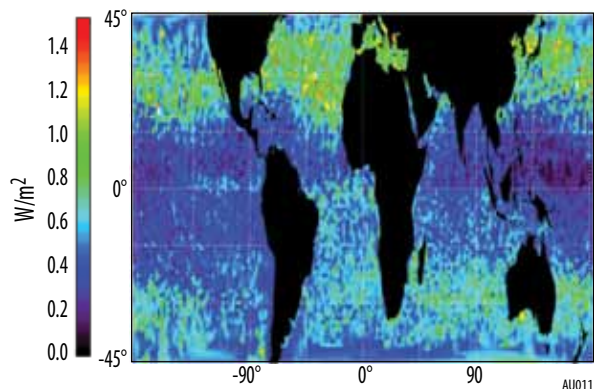


Figure 14: Annual average clear-sky OLR reduction estimated from TES upper tropospheric (200-500 hPa) O₃. Measurement uncertainties correspond to ~1 color bar gradation.

compassing a broad range of variability from climate nodes (such as El Niño's, the Arctic Oscillation, and MJO), is essential for validating climate models to improve predictability of future climate.

3.4 A-Train Science

The A-Train is a popular term for the close orbiting afternoon constellation of satellites, Aqua, CloudSat, CALIPSO, Parosol and Aura. The various instruments on the A-Train provide a more comprehensive remote sensing capability than any single platform. For example, while Aura TES and Aqua AIRS measure roughly the same IR spectral range, AIRS has a wider swath and TES has higher spectral resolution. Aura was initially positioned in orbit ~15 minutes behind Aqua. This was the minimum separation possible because the antennas at Svalbard could not downlink the satellite X-Band transmissions within 15 minutes. Upgrades have made near-simultaneous downlink of Aura and Aqua data possible. The Project Science Office recommended reducing the time gap between Aqua and Aura, also improving the coincidence between MLS and CALIPSO/CloudSat measurements. NASA HQ approved this change in position and Aura is now positioned (completed in 2008) ~7 minutes behind Aqua.

MLS measurements of Ice Water Content (IWC) complement those from CloudSat and CALIPSO. CloudSat is sensitive to thick larger-particle clouds, CALIPSO is sensitive to aerosols and thin clouds. MLS's 640GHz and 2.5THz radiometers are sensitive to upper tropospheric cirrus that are generally too tenuous to be observed by CloudSat but too opaque to be fully penetrated by the CALIPSO lidar [Wu *et al.*, 2008b]. Thus, the three instruments are highly complementary. MLS can obtain cloud particle habit (shape/alignment) information through observations

at different polarizations [Davis *et al.*, 2005]. Kahn *et al.* [2007] performed a detailed comparison of MLS, AIRS and CALIPSO observations of cloud properties, a step towards building a comprehensive 3-D picture of upper tropospheric cloud structure. Work (funded through a ROSES proposal) is ongoing to combine OMI optical cloud centroid pressures with IR cloud-top pressure from MODIS to detect multi-layered/phase clouds and identify optically thick clouds over snow/ice [Joiner *et al.*, 2009b].

Studies of the impact of aerosols on cloud properties (the so-called aerosol indirect effects that represent critical uncertainties in climate modeling) are hampered by the lack of measurements of aerosols in the presence of clouds. The ability of MLS to measure CO - a pollutant that often accompanies aerosol - in the presence of cloud represents a powerful new tool for such studies. Jiang *et al.* [2008] have demonstrated a reliable correlation between MLS CO and MODIS aerosol observations in selected regions and seasons. By using MLS CO as a proxy for pollution aerosol in cloudy regions, the authors showed that polluted clouds are associated with smaller particle sizes (from MODIS) and weaker precipitation (from TRMM) than 'clean' clouds (Figure 15). A wide variety of studies of these important processes will be enabled by the MLS observations and their co-location with observations from other instruments in the A-train.

A-train satellite measurements of aerosols, clouds, ozone, carbon monoxide, and bromine from MODIS, CALIPSO, CloudSat, AIRS, and the Aura instruments TES, MLS, and OMI have been integrated with aircraft into several atmospheric chemistry campaigns such as ARCTAS, INTEX-B, and TexAQS 2006. The satellite measurements were used for aircraft flight planning and subsequent analysis for understanding the sources, evolution, and transport of pollution plumes [e.g. Cowling *et al.*, 2007; Zhang *et al.*, 2008; Pierce *et al.*, 2009].

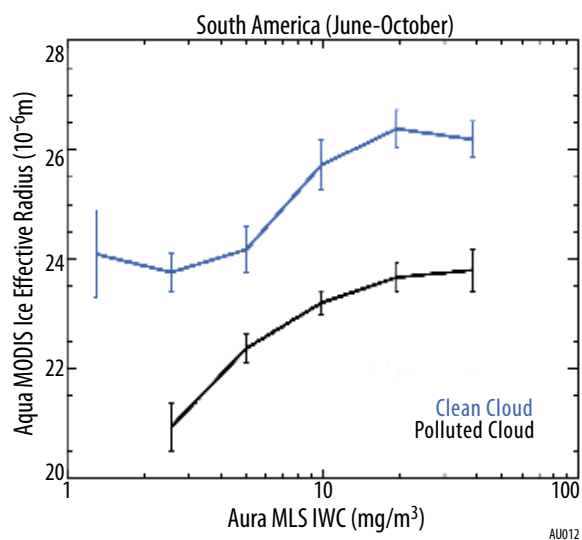


Figure 15: The relationship between the MODIS cloud effect particle size and MLS cloud ice water content differs for clean and polluted clouds. MLS CO is less than 120 ppbv for 'clean' clouds and greater than 240 ppbv for polluted clouds. The error bars indicate confidence in the mean. Adapted from Jiang *et al.* [2009].

3.5 Relevance to Modeling and Prediction

Improving the predictive capability for changes in the ozone layer, climate forcing and air quality is an element of NASA's strategic plan, thus use of Aura data for model development and evaluation is key to the success of the Aura mission. MLS daily global observations of cloud ice water content (IWC) profiles, the first of such kind before the launch of CloudSat, are being used to explore the causes for disagreements of as high as factors of 20 among IWC estimates from state-of-the-art climate models. Comparisons with MLS observations [Li *et al.*, 2005b] have guided model improvements. Subsequent studies [Li *et al.*, 2007] showed a low bias in ECMWF IWC that progressively worsens when the model is run in forecast mode. Su *et al.* [2006a, 2006b] studied the relationships between MLS H₂O, MLS cloud ice, and SST, comparing them to relationships predicted by 15 climate models and showing model/data differences are as large as 400%. These studies point to the inadequacy of the cloud physics parameterization in many of the models being used for climate prediction. High clouds, like cirrus, have a net positive global warming effect and the failure of the models to predict the IWC in the tropical upper troposphere is a serious concern. However the new data

from MLS and CloudSat allow modelers to focus on this process and correct the cloud parameterizations.

Stratospheric chemistry models must be able to make quantitative assessments of polar ozone depletion as described in Section 3.1. For polar ozone depletion, parameterizing the formation of polar stratospheric clouds is necessary since the total area of cloud surface area is proportional to the ozone depletion for constant stratospheric chlorine [Rex *et al.*, 2006; Douglass *et al.*, 2006]. PSCs are optically thin but are detectable by HIRDLS [e.g., Massie *et al.*, 1998] and CALIPSO. Because the PSCs are formed by condensation of HNO₃ and H₂O and because the chemical transformations affect HCl and ClO, MLS constituent measurements are central to model evaluation of polar processes. Pitts *et al.* [2007] compare estimates of PSC areal coverage during the 2006 Antarctic winter from CALIPSO with temperature-based proxies of PSC formation derived using MLS profiles of HNO₃ and H₂O. Santee *et al.* [2008a] investigated variability in lower stratosphere chlorine partitioning using MLS data with ClONO₂ from the ACE-FTS and showed that the SLIMCAT 3D CTM overestimated the magnitude, spatial extent, and duration of chlorine activation, in part because of the equilibrium scheme used to parameterize PSCs.

Aura measurements of lower stratospheric constituents are being used to evaluate simulated transport and mixing in various models used to assess stratospheric ozone depletion. For example, HIRDLS frequently observes thin layers of O₃ and HNO₃ in the northern middle latitude lower stratosphere during winter and spring; these layers require 1-2 km vertical resolution. Yudin *et al.* (2009b) showed the necessity of addressing the consistency of the vertical scale of observations and models in ozone assimilation studies. Models that cannot reproduce the formation of these layers have inadequate transport processes because these layers contribute to variability in the lower stratospheric ozone [Douglass *et al.*, 2008; Gille *et al.*, 2008].

The tropospheric chemistry measurements of Aura are being used to find the model errors in global tropospheric chemical transport models. These models have been primarily tested against ground based measurements at limited locations, aircraft measurements over limited time periods, or with remote sensing measurements with little vertical information or sensitivity to the troposphere. The measurements of Aura now provide information about the vertical distribution of ozone and let us check the representation of the complex tropospheric processes, such as upper tropospheric ozone formation. As described in Section 3.2.4, TES observations are now being assimilated in a number of models. For example, using data assimilation techniques, Parrington *et al.* [2008] constrained ozone predictions from GEOS-CHEM and AM2-Chem during the summer of 2006 with TES observations. These models under-predicted mid-tropospheric ozone by as much as 40% and were corrected to within 5% of independent ozone-sonde measurements after assimilating the TES satellite measurements. Water vapor isotope measurements from TES are used in ROSES funded work to assess water process representation in the NCAR CAM and GISS models. Finally, ROSES funded research

is now supporting multi-chemistry/climate model comparisons between the ozone radiative forcing of TES and the AM2-Chem, GISS, CAM-Chem, and ECHAM5-MOZ models. If successful, these comparisons could be included in the upcoming IPCC Assessment Report (AR) 5.

In summary, Aura data have been used to test and constrain the physics in models of cloud and ice formation and to test the chlorine chemistry, including the possibility of a much slower dimer photolysis than the standard value. High resolution observations of temperature and trace species are being used to evaluate transport pathways and mixing processes that are critical to the ozone budget in the climatically important UTLS region. Aura data are being assimilated in models to evaluate chemical and dynamical processes. These studies have revealed model areas in need of improvement, and will lead to better understanding of physical, chemical and dynamical processes.

4.0 THE AURA EXTENDED MISSION PROPOSAL

Continuation of the Aura mission supports the study of Earth's atmosphere and contributes specifically to the NASA research objective to 'Understand and improve predictive capability for changes in the ozone layer, climate forcing, and air quality associated with changes in atmospheric composition.' Aura achievements during the primary mission phase have been substantial (as indicated above). The overall goal for Aura's continued mission is to continue the long term record of atmospheric trace gases and measure constituent variations under an increasing variety of natural and man-made conditions which allow us to better separate and quantify the factors controlling these processes. For example, we are already seeing changes in tropospheric trace gases associated with the global economic downturn. An extended observation record, encompassing additional natural and man-made changes in climate conditions, air quality emissions and the solar cycle, will strengthen the observational and theoretical foundation of Earth system understanding and improve predictive capability of models.

MLS, OMI and TES are all presently operational and will contribute to the extended mission by continued measurements, algorithm improvements, retrieval of additional species and analysis as discussed in more detail below. In the event that the HIRDLS chopper does not restart, the HIRDLS contribution to the Aura extended mission will be limited to algorithm development to improvement of present retrievals in order to recover additional species. In the event of a chopper restart, HIRDLS will contribute more substantially as detailed in Section 5.4.

4.1 Is the O₃ Layer Changing as Expected?

Atmospheric abundances of ozone depleting substances are declining, although complete 'recovery' in stratospheric ozone (including the Antarctic ozone hole) is not expected for decades. Monitoring the changing stratospheric chemistry is a key goal of the Aura mission and a Congressional mandate for NASA. Currently only two satellite instruments can measure stratospheric chlorine (HCl), the most important chlorine reservoir: MLS on Aura and ACE on the Canadian SciSat satellite (Figure 5). SciSat was a three

year mission launched in 2003 and is already in extended operations. Only Aura's MLS has the resources to make ongoing measurements of stratospheric chlorine into the next decade – a chlorine record begun by UARS in 1991. It is also important to note that only MLS, ACE, MIPAS (on Envisat, launched in 2002) provide the additional trace gases needed to assess stratospheric chemistry. Envisat is also in extended mission operations. Continued Aura measurements will lengthen the trend quality data set for total O₃ (OMI) and also lengthen the records for other constituents such as HCl and H₂O that are important to O₃ (MLS). Continued observations from MLS expand the data base of global tracer profiles (e.g., N₂O and, in many circumstances, H₂O) needed to quantify northern hemisphere variability. Accounting for variability makes it possible to remove 'dynamic contribution' to O₃ trends, making the changes derived for chlorine changes more reliable and will contribute to nascent efforts to detect and quantify change in the stratospheric overturning circulation that is predicted by current models [Butchart *et al.*, 2006]. Continuing the column ozone data record will lengthen the stratospheric observations begun by the TOMS series (1979 ->).

4.2 What are the Processes that Control Tropospheric Pollutants?

The overall goal of the extended Aura mission pollution measurements is to characterize the changes in production of short- and long-lived gases, aerosols, and their long-range transport under a variety of climatic and economic conditions. A continued record of pollution gases is critical because emission changes related to climate (e.g., biomass burning frequency and intensity, temperature driven soil and vegetation emission), and emission changes from anthropogenic sources (e.g., related to population growth, economic growth and shrinkage, environmental regulation) have comparable magnitudes. Improved emission estimates are crucial to improve model predictions for air quality and climate. Measurements made by OMI and TES can improve the emission estimates of several of the trace gases. For example, the mild El Niño of 2006 produced significant increases in VOCs, CO, and NO₂ (observed with TES and OMI) as a result of intense fires and degraded air quality throughout the tropical Pacific region. Tropospheric O₃ was affected by increases in these precursors as well as changes in the distribution lightning generated NO_x [Logan *et al.*, 2008; Chandra *et al.*, 2009]. Extended global observations of such processes and evaluations of chemical-transport over a wide range of conditions will allow for improved separation of local and long-range effects on air quality. This will enable better prediction of the potential global and regional impacts of emissions increases in a changing climate.

Significant reductions in short-lived tropospheric NO₂ have been observed with OMI over the US between 2005 and 2007 as shown in **Figure 16**. This is the result of increased emission controls on vehicles and power plants. At the same time, large NO₂ increases were observed over southeast Asia. Witte *et al.* [2009] report measurable decreases in NO₂ and other pollutants over Beijing during the 2008 Olympic games as a result of localized emission con-

trols. OMI retrievals of boundary layer SO₂ in the Middle East are correlated with gasoline prices as refining capacity changes [S. Carn, personal communication]. The impact of hurricanes Katrina and Rita on the oil industry and shipping lead to decreases in NO₂ concentrations in the Gulf of Mexico as seen by OMI [Yoshida *et al.*, 2009]. The high spatial resolution and sampling provided by OMI allows for significantly improved identification and quantification of such emission changes as compared with lower resolution UV/Vis instruments. The impact of the current economic crisis on pollutant emissions should be discernable by OMI (TOR, NO₂, SO₂, VOCs) as well as TES (O₃, CO) and will allow us the opportunity to further baseline pollution emissions as a function of economic activity.

Ammonia (NH₃) and methanol (CH₃OH) will be added to the suite of TES core products under the extended mission proposal. **Figure 17** shows an example of TES NH₃ concentrations near Beijing [Beer *et al.*, 2007]. NH₃ is important to both air quality and climate as it contributes to aerosol formation. Global NH₃ concentrations are highly uncertain in part because NH₃ is difficult to measure *in situ*. TES NH₃ will contribute to the development

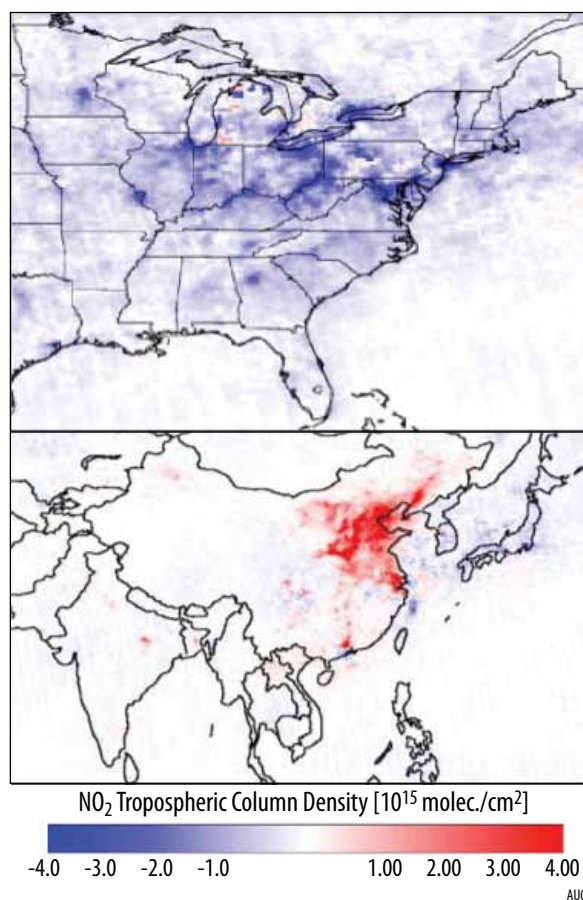


Figure 16: The annual mean difference in tropospheric NO₂ column between 2007 and 2005 showing trends in the eastern United States (top) and Asia (bottom). Blue (red) shows significant decreases (increases) NO₂ with time. (courtesy Geert Vinken, TUE, and Folkert Boersma, KNMI)

of global, time-dependent emission constraints. Methanol is the most abundant oxygenated hydrocarbon gas in the atmosphere [Singh *et al.*, 1995]. Estimates of global emissions are highly uncertain with disagreement about whether the marine biosphere or plant growth are the main sources [Millet *et al.*, 2008]. Global CH₃OH measurements from TES could significantly reduce the uncertainty in the global budget and help resolve controversy about their sources and concentrations.

Future tropospheric ozone trends are important to quantify and explain. As described in Section 3.2.4, Zhang *et al.* [2008], suggest that the doubling of Asian emissions as observed by OMI NO₂ observations from 2000 to 2006 result in 1-2 ppbv increase in background ozone concentrations in western North America. Using data over 20 years, Parrish *et al.* [2009] found a trend in ozone from marine boundary layer inflow on the West coast of 0.34 ppbv ± 0.09 ppbv/yr, which cannot be reproduced by current transport and chemistry models. These data are limited to surface observation sites and therefore do not have sufficient coverage to constrain the range of processes that may be responsible for these trends. Global remote sensing measurements taken over longer times scales are vital to disentangle the relative contribution of emissions, climate, and chemistry to these observed trends.

4.3 What are the Roles of UT Aerosols, Water Vapor and Ozone in Climate Change?

The upper troposphere (UT) is a critical region of the atmosphere for climate stability. It is here where water vapor (the strongest greenhouse gas – GHG) and ozone (also a strong GHG in this region) have their largest radiative forcing. In addition, the net radiative forcing of UT clouds is a delicate balance between short wave cooling and long wave heating. The processes that control the budgets of UT GHGs are many and complex. Aura measurements are

unique in providing daily global upper tropospheric observations of ozone with a vertical resolution needed to better quantify these processes and their impacts.

4.3.1 Water Vapor, Clouds and Aerosols Issues

MLS cloud and water vapor observations have, as described above, been used to quantify cloud and water vapor feedbacks, and improve parameterizations of cloud processes in weather and climate models. Continued observations of these processes, including their modulation by phenomena such as El Niño, will provide information needed to further validate and improve these models. An important goal of the Aura extended mission is to capitalize on the unique scientific opportunities presented by the A-train satellites. In particular, the Aura orbit was changed in 2008 to give better collocation between MLS and CloudSat/CALIPSO observations. This, combined with new MLS cloud products under development (described below) and OMI cloud pressures, will enable new unified studies of cloud. This new information, when combined with the MLS observations of CO pollution within clouds, will enable better quantification of aerosol/cloud interactions.

Cirrus clouds are extremely important to Earth's radiation budget, especially in the tropics. Future improvements to the HIRDLS algorithm will improve the detection and characterization of atmospheric particulates. This information will be combined with that obtained from simultaneous retrieval of temperature and water vapor to improve our models of cirrus microphysics.

TES observations of the isotopic composition of water vapor are being used to quantify the global distribution of evaporation and condensation processes affecting the distribution of water vapor [e.g., Worden *J. et al.*, 2007, Brown *et al.*, 2008]. Observing how the distribution of these moisture sources and sinks is affected by climate modes such as El Niño, the Arctic Oscillation, and the MJO is key for understanding how future variations in climate will affect global precipitation patterns.

4.3.2 Changes in Stratospheric Dynamics

Model studies indicate that the stratospheric Brewer Dobson Circulation (BDC – the stratospheric cycle of upwelling in the tropics, poleward transport aloft and downwelling in polar regions) may be speeding up in response to changing climate, potentially significantly modifying the timing of ozone layer recovery. Global atmospheric composition observations are a proven tool for diagnosing slow atmospheric motions such as the BDC [Schoeberl *et al.*, 2008a]. Continued Aura MLS daily global measurements of long-lived tracers (e.g., N₂O and H₂O) from the tropopause to the mesosphere, are critical for diagnosing the BDC, its variability and evolution. Changes in the BDC may also be visible in the total ozone and profile measurements of OMI and MLS. This analysis will be augmented by HIRDLS measurements of CF₂Cl₂ and CFCl₃ (already released) as well as CH₄ that will be released in the next version of their algorithm.

The temperature and dynamics of the upper stratosphere and lower mesosphere (US/LM) are also sensitive indicators of climate change [e.g., Rind *et al.*, 1998, Manzini *et al.*,

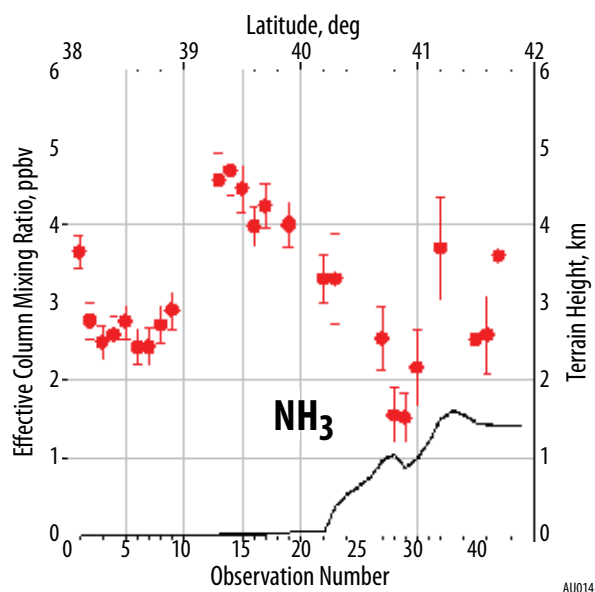


Figure 17: Ammonia concentrations estimated from TES radiance residuals over Beijing measured on July 10, 2007.

[2003]. An extended daily global observation record in this region from Aura will help validate the depiction of US/LM processes in climate models, improving our ability to identify and diagnose climate change ‘fingerprints’. MLS mesospheric temperature and humidity observations also provide important information on Polar Mesospheric Clouds, one such climate change fingerprint [Morris *et al.*, 2009].

The HIRDLS H₂O product with ~1 km vertical resolution will enable more accurate quantification of the processes controlling upper tropospheric humidity especially in the tropics. **Figure 18** shows preliminary results for HIRDLS H₂O compared to MLS. Overall there is reasonable agreement but the differences show the temporal dependence in the HIRDLS radiance correction and the need for improving the algorithm. These improvements are being developed now and are projected to be implemented in the next algorithm release.

4.3.3 Upper Tropospheric Radiative Forcing

Quantification of the radiative forcing from tropospheric ozone is challenging because of the sensitivity of ozone to many poorly characterized processes (convection, transport, stratospheric influx, chemistry), its comparatively short lifetime, and a relative lack of observations. Natural and anthropogenic processes contribute to upper tropospheric ozone, and separating the radiative forcing due to man-made processes from that due to natural processes is an additional challenge. Furthermore, short term climate variations will alter the distribution of these radiatively active gases and currently we have very limited information on interannual variability in radiative forcing.

“All-sky” vertical ozone instantaneous radiative forcing (IRF) – the effect of upper tropospheric ozone on the radiative balance of the atmosphere – from TES will provide

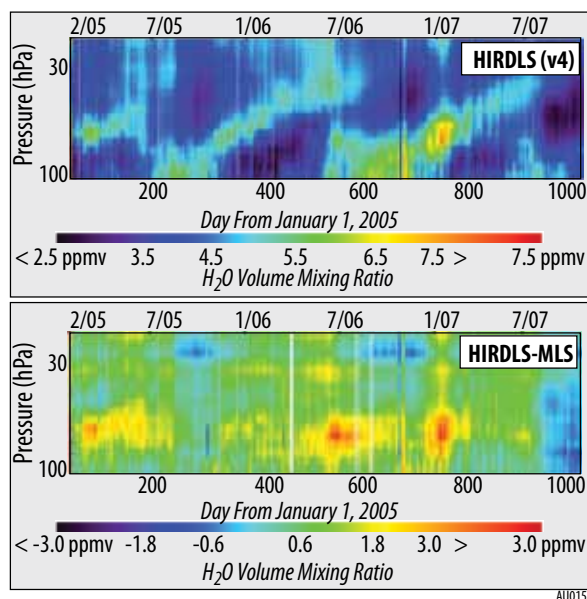


Figure 18: HIRDLS observations of the tropical water vapor tape recorder (top) and the difference between the MLS water vapor tape recorder and the HIRDLS tape recorder (bottom).

a new observational constraint on the ozone greenhouse impact on climate. This product will allow us to quantify changes in this forcing as a function of both natural and man-made conditions. TES IRF can distinguish the effects of ozone, water vapor, and clouds on outgoing longwave radiation in the ozone band. This will enable quantification of impact of vertical distribution of ozone on radiative forcing. Comparisons with TES IRF should enable improvements in climate model representations of ozone radiative forcing. Tropospheric ozone can also be derived from OMI and can also be used to calculate its radiative forcing component [Joiner *et al.*, 2009a]. As describe in Section 3.3.2, ROSES funding is being used to begin intercomparisons of the ozone radiative forcing of TES and the AM2-Chem, GISS, CAM-Chem, and ECHAM5-MOZ models.

4.3.4 Climate Impact of Volcanoes

Volcanoes not only pose significant risks to aircraft and local populations, but also have a potentially large climate impact, as emitted SO₂ converts to sulfate aerosols which have a long lifetime in the stratosphere. Anthropogenic SO₂ similarly contributes to aerosol formation in the troposphere. The climate effects of high latitude volcanoes are highly uncertain [J. Hansen, personal communication, 2009]. The 2008 Kasatochi and Okmok Alaskan eruptions were the first major high latitude events since Aura launched. Kasatochi deposited ~1.5M-tons of SO₂ into the atmosphere. The plumes spread throughout the northern hemisphere within 20 days as shown in **Figure 19**. The decay of the total volume of SO₂ with time suggests that the SO₂ was quickly converted to sulfate aerosol. Currently there is no instrument monitoring the stratospheric sulfate layer so we can only infer the climate impact from the layer after it becomes too thin for CALIPSO to measure. The combination of OMI and CALIPSO data is critical for monitoring the climate impact of volcanic eruptions that reach stratospheric altitudes.

5.0 PROPOSED AURA EXTENDED MISSION IMPLEMENTATION PLAN

Here we discuss the core activities with a focus on al-

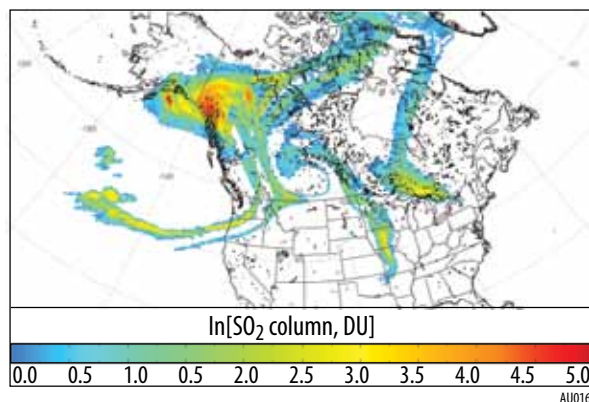


Figure 19: SO₂ plumes (on a logarithmic color scale) as observed with OMI on 12 August 2008 following the eruption of the Alaskan Kasatochi volcano.